HHS Public Access

Author manuscript

Toxicol Appl Pharmacol. Author manuscript; available in PMC 2023 August 15.

Published in final edited form as:

Toxicol Appl Pharmacol. 2022 August 15; 449: 116137. doi:10.1016/j.taap.2022.116137.

Biological effects of inhaled crude oil vapor V. Altered biogenic amine neurotransmitters and neural protein expression

Krishnan Sriram[*],
Gary X. Lin,
Amy M. Jefferson,
Walter McKinney,
Mark C. Jackson,
Jared L. Cumpston,
James B. Cumpston,
Howard D. Leonard,
Michael L. Kashon,
Jeffrey S. Fedan

Health Effects Laboratory Division, National Institute for Occupational Safety and Health, Morgantown, WV 26505, United States of America

Abstract

Workers in the oil and gas industry are at risk for exposure to a number of physical and chemical hazards at the workplace. Chemical hazard risks include inhalation of crude oil or its volatile components. While several studies have investigated the neurotoxic effects of volatile hydrocarbons, in general, there is a paucity of studies assessing the neurotoxicity of crude oil vapor (COV). Consequent to the 2010 Deepwater Horizon (DWH) oil spill, there is growing concern about the short- and long-term health effects of exposure to COV. NIOSH surveys

[*]Corresponding author at: Toxicology and Molecular Biology Branch, National Institute for Occupational Safety and Health, 1000 Frederick Drive, Mailstop L-3014, Morgantown, WV 26508, United States of America. kos4@cdc.gov (K. Sriram).

Disclaimer

The findings and conclusions in this report are those of the author(s) and do not necessarily represent the official position of the National Institute for Occupational Safety and Health, Centers for Disease Control and Prevention.

Supplementary data to this article can be found online at https://doi.org/10.1016/j.taap.2022.116137.

Credit author statement:

Credits

Krishnan Sriram: Conceptualization, Methodology, Investigation, Data Analysis, Data curation, Writing (original, review and editing).
Gary X. Lin: Methodology (neurotoxicity studies), Investigation (neurotoxicity studies).
Amy M. Jefferson: Methodology (neurotoxicity studies), Investigation (neurotoxicity studies).
Walter McKinney: Methodology (inhalation system design), Software (system operations).
Mark C. Jackson: Methodology (inhalation system design), Software (system operations).
Jared L. Cumpston: Investigation (inhalation exposures).
James B. Cumpston: Investigation (inhalation exposures). Howard D. Leonard: Investigation (inhalation exposures).
Michael L. Kashon: Formal Data Analysis.
Jeffrey S. Fedan: Conceptualization, Data curation, Writing (review & editing), Project administration, Funding acquisition.

Data statement

Study data will be available in public domain at the NIOSH Data and Statistics Gateway after final publication of the article.

Declaration of Competing Interest

The authors declare that they have no conflicts of interest in relation to this publication.

suggested that the DWH oil spill cleanup workers experienced neurological symptoms, including depression and mood disorders, but the health effects apart from oil dispersants were difficult to discern. To investigate the potential neurological risks of COV, male Sprague-Dawley rats were exposed by whole-body inhalation to COV (300 ppm; Macondo surrogate crude oil) following an acute (6 h/d × 1 d) or sub-chronic (6 h/d × 4 d/wk. × 4 wks) exposure regimen. At 1, 28 or 90 d post-exposure, norepinephrine (NE), epinephrine (EPI), dopamine (DA) and serotonin (5-HT) were evaluated as neurotransmitter imbalances are associated with psychosocial-, motor- and cognitive-disorders. Sub-chronic COV exposure caused significant reductions in NE, EPI and DA in the dopaminergic brain regions, striatum (STR) and midbrain (MB), and a large increase in 5-HT in the STR. Further, sub-chronic exposure to COV caused upregulation of synaptic and Parkinson's disease-related proteins in the STR and MB. Whether such effects will lead to neurodegenerative outcomes remain to be investigated.

Keywords

Brain; Inhalants; Inhalation studies; Neurological disorders; Neurotoxicity; Neurotoxicology; Occupational exposure limits; Oil and gas; Parkinsonism; Psychosocial; Toxicology; Volatile organic compounds

1. Introduction

This is the fifth paper in a series of seven papers which focus on an investigation of the effects of inhaled crude oil vapor (COV) (McKinney et al., 2022) on the pulmonary, cardiovascular, nervous, and immune systems (Fedan et al., 2022; Sager et al., 2022; Krajnak et al., 2022; Weatherly et al., 2022) using an animal model. The purpose of the overall investigation is presented in the introductory paper (Fedan, 2022) and a summary of the findings are compiled in the concluding paper (Investigative Team, 2022).

In the oil and gas industry, workers are potentially exposed to crude oil or COV during upstream operational processes like drilling and extraction, midstream activities like transportation and storage, as well as downstream activities like refining (Verma et al., 2000; Esswein et al., 2014; Harrison et al., 2016; Retzer et al., 2018). Worker exposure to various fractions of crude oil have been linked to musculoskeletal, respiratory, gastrointestinal, circulatory problems (Valentic et al., 2005), and cancer (Divine and Barron, 1987); Schnatter et al., 1992; Sathiakumar et al., 1995; Wong and Raabe, 2000; Divine and Hartman, 2000; Kirkeleit et al., 2008; Stenehjem et al., 2014). Mortality has also been reported among the oil and gas extraction workers with acute hydrocarbon inhalation while opening the thief hatches of oil storage tanks as a possible contributing factor (NIOSH, 2015).

The explosion of the Deepwater Horizon (DWH) oil drilling rig in April 2010 resulted in the largest offshore oil spill catastrophe. Approximately 210 million gallons (5 million barrels) of crude oil was reported to have been discharged into the Gulf of Mexico (McNutt et al., 2012). The oil spill response action involved recruitment of nearly 48,000 response workers, including about 8700 U.S Coast Guard personnel, to contain and clean up the spill (Rusiecki et al., 2018a). The cleanup workers were exposed to a variety of chemical hazards that could potentially increase the risk of short- and long-term adverse health outcomes

(Rusiecki et al., 2018b). These included exposures to chemical components of the crude oil, including, volatile organic compounds (VOCs), polycyclic aromatic hydrocarbons, and heavy metals, as well as components of the dispersants employed to disperse the oil. The Gulf Long-term Follow-up Study of the DWH oil spill response workers reported that exposure to low doses of benzene and other volatile organic compounds such as toluene, ethylbenzene, oxylene, xylene, and styrene, are associated with adverse hematologic effects (Doherty et al., 2017). Another long-term follow-up study of the oil spill response personnel also showed that the workers involved in the cleanup operations experienced prolonged and/or progressive worsening of their hematological profile, as well as pulmonary, hepatic and cardiac functions (D'Andrea and Reddy, 2018).

A recent cross-sectional study of the U.S Coast Guard personnel involved in the DWH oil spill response identified acute neurological symptoms associated with crude oil exposure or co-exposure to both crude oil and the oil dispersant used in the clean-up operations (Krishnamurthy et al., 2019). The study reported that the U.S. Coast Guard personnel experienced headache, dizziness, concentration problems, and memory loss/confusion following inhalation of crude oil and/or oil dispersant, which exhibited an exposure-response relationship. The authors further suggested that the acute neurological symptoms examined showed moderate to strong correlation among each other, and thus the observed elevated risks may reflect a common neural mechanism (Krishnamurthy et al., 2019). These findings, while of great importance, could not inform regarding the neurotoxicity of COV itself during the co-exposure, which was the purpose of the present investigation.

NIOSH Health Hazard Evaluation (HHE) surveys among the cleanup workers identified a variety of health effects, including neurological symptoms (King and Gibbins, 2011). Unfortunately, as a significant number of response workers who experienced health symptoms were exposed to both crude oil and the oil dispersant that was aerially sprayed to contain the spill, the health effects of crude oil exposures alone were difficult to discern from these surveys. It is here that laboratory-based studies are advantageous as they can provide ample health risk information to establish the toxicological potential of the various chemical hazards at the workplace. To that end, we previously showed that acute inhalation of the oil dispersant COREXIT® EC9500A elicited neurotoxicity in an experimental animal model (Sriram et al., 2011). In continuation of the efforts to characterize the neurotoxic potential of COV in upstream workers in the oil and gas industry in general, and in oil spill cleanup workers, the present work evaluated the neurotoxic risks following exposure to COV generated from Macondo well crude oil that was used as a surrogate for the DWH crude oil. Such efforts will ultimately contribute towards development of appropriate pre-job planning protocols, exposure assessment and biomonitoring procedures, development of appropriate personnel protective equipment, and possible establishment of occupational exposure limits for crude oil based on neurotoxicity risk.

2. Methods

2.1. Animals

Male Sprague-Dawley [Hla:(SD) CVF] rats (200–225 g; 40–45 days of age) were procured from Hilltop Lab Animals (Scottdale, PA). Upon arrival, animals were housed

in pairs in ventilated micro-isolator units with autoclaved ALPHA-dri® virgin cellulose chips (Shepherd Specialty Papers; Watertown, TN) and hardwood Beta-chips (NEPCO; Warrensburg, NY) for bedding, with provision for HEPA-filtered laminar flow air (Thoren Caging Systems; Hazleton, PA). Tap water and Harlan 2918 irradiated Teklad Global 18% rodent chow (Harlan Teklad; Madison, WI) was provided *ad libitum*. Rats were housed under controlled light cycle (12 h light/12 h dark), temperature (22–25 °C) and humidity (40–65% RH) conditions. The NIOSH animal facility is specific pathogen-free, environmentally controlled, and accredited by AAALAC International. All animals were acclimated for at least 6 d after arrival prior to experimentation. All animal use and procedures have been reviewed and approved by the Institutional Animal Care and Use Committee.

2.2. Whole-body inhalation exposure to COV

COV was generated using Macondo well surrogate crude oil obtained from the Gulf of Mexico. The Macondo well is in close proximity to the DWH oil spill site. The COV was well characterized prior to use in animal exposures (McKinney et al., 2022). An automated whole-body inhalation exposure system was developed to expose animals to COV (McKinney et al., 2022). Briefly, COV was generated using a collision type atomizer. Chamber concentration and pressure were regulated with software feedback loops to ensure that constant concentrations of COV (300 ppm × 6 h/d) were maintained throughout the duration of the exposure. Additionally, Benzene, Toluene, Ethylbenzene, Xylene (BTEX) gases, temperature, humidity, and carbon dioxide levels were monitored throughout the duration of the whole-body inhalation exposure. The COV concentration chosen for the study is comparable to that reported in the breathing zone of workers conducting upstream operations in the oil and gas industry (Verma et al., 2000; NIOSH, 2015).

Prior to exposures, rats were acclimated in the inhalation chamber for 4–5 d. During inhalation exposures, the animals were housed individually inside stainless-steel wire mesh cages. The dimensions of individual cells in the cages are adequate to provide the animal sufficient room without confining them to an abnormal environment during exposure and provide unobstructed airflow. The chamber air flow was maintained at 40–50 L/min with 8–12 air changes/h to keep carbon dioxide levels under 4000 ppm. The chamber temperature was maintained between 66 and 79 °F (usually 72 °F) and the chamber relative humidity was maintained between 35 and 60% (usually 45%).

Rats were exposed by whole-body inhalation to 300 ppm of COV aerosol for 6 h/d for one of two durations: a single exposure for one day (300 ppm; 6 h/d × 1 d; acute exposure), or a repeated exposure of 4 d/ wk. for 4 consecutive wks (300 ppm; 6 h/d × 4d/wk. × 4 wks; for a total of 16 d; sub-chronic exposure). Control animals were simultaneously exposed to HEPA-filtered air in an identical exposure system.

The exposures were conducted in two experimental blocks to obtain a final $n = 8$ for each experimental group. During the daily 6 h whole-body inhalation exposures, the animals did not have access to food or water. Animals exposed under such conditions did not exhibit any observable pain or distress, body weight changes, behavioral abnormalities or adverse health effects.

2.3. Euthanasia and sample collection

In the acute COV exposure studies, animals were euthanized at 1 or 28 d after exposure. In the sub-chronic COV exposure studies, animals were euthanized at 1, 28 or 90 d after cessation of exposure. Euthanasia was performed by administration of sodium pentobarbital euthanasia solution (Fatal Plus; >100–300 mg/kg; Vortech Pharmaceutical Ltd., Dearborn, MI; intraperitoneal injection), and the animals were exsanguinated by transecting the abdominal aorta to ensure death. All euthanasia and tissue collection procedures were performed between 7:30–11:30 am on the days of the sample collection. After euthanasia and collection of lung lavage fluid for pulmonary toxicity assessment (Sager et al., 2022), the brains were excised and discrete brain areas, *i.e.*, olfactory bulb (OB), striatum (STR) and midbrain (MB) from the left and right hemispheres, were dissected free-hand. Tissues from the right hemisphere were collected in 1% perchloric acid and stored at − 75 °C until processing for biogenic amine neurotransmitter analysis. Tissues from left hemisphere were collected in Tissue Protein Extraction Reagent (T-PER, Pierce Biotechnologies, Inc.; Rockford, IL) containing protease inhibitor cocktail and EDTA for subsequent isolation of protein for immunoblot analysis. Due to the cellular heterogeneity of the nervous system, as well as the progressive nature of neural injury, the timeline of expression of various injury markers (neurotransmitters, neuronal and synaptic proteins, glial proteins) are distinct. Through a careful understanding of the time course of expression of various neural makers based on our previous experience (Sriram et al., 1997, 1998, 2004, 2011, 2020), we monitored their changes at relevant time points in this study. As synaptic and neuronal damage are typically delayed events, changes in their protein markers were monitored at 28 d after the acute exposure and all post-exposure time points after the sub-chronic exposure. Changes in neurotransmitters were monitored at all post-exposure time points after acute and sub-chronic exposures in order to determine both early and long-term/persistent alterations in their levels.

2.4. Measurement of biogenic amines in brain tissue by high performance liquid chromatography with electrochemical detection (HPLC-EC)

The biogenic amines, norepinephrine (NE), epinephrine (EPI), dopamine (DA), and serotonin (5-hydroxytryptamine, 5-HT), and the metabolites of DA and 5-HT namely, 3,4-dihydroxyphenylacetic acid (DOPAC); homovanillic acid (HVA); and 5-hydroxyindole-3-acetic acid (5-HIAA), were measured by HPLC-EC (Sriram et al., 2014). Briefly, brain tissues (OB, STR, MB) were homogenized in 1% perchloric acid containing isoproterenol (as internal standard) and centrifuged for 10 min at 12,000 × *g*. The supernatant was filtered through a 0.2 μm nylon filter and 10 μL aliquots were injected onto a C-18 reverse phase HPLC column (Agilent Technologies; Santa Clara, CA) using an UltraFast Liquid Chromatography (UFLC) system (Shimadzu Instruments; Columbia, MD) attached to an autosampler. A BAS-LC4B amperometric detector (BASi Inc.; West Lafayette, IN) with a glassy carbon oxidative flow cell was used for detection at an electrode potential of 0.8 V. The mobile phase (pH 3.2) consisted of 0.15 M monochloroacetic acid, 0.115 M sodium hydroxide, 0.1 mM EDTA, 0.015% sodium octyl sulfate, 3% acetonitrile, 1.5% methanol and 1.2% tetrahydrofuran. Under these conditions NE, EPI, DA, 5-HT were chromatographically separated and detected. Analytes were quantified by comparing peak area detector responses in the sample with those produced by a series of standards

similarly prepared in 1% perchloric acid. The pellet from each of the processed samples was solubilized with 3% sodium hydroxide and the protein content was estimated. The neurotransmitter content in each sample was then normalized to the amount of protein. The values were calculated as ng/mg total protein and are graphically represented as percent of air-exposed controls.

2.5. Preparation of brain tissues for protein isolation

Brain tissues (OB, STR, MB) collected in 1.5 mL microfuge tubes were homogenized using 0.3 mL of T-PER tissue protein extraction reagent (Pierce Biotechnologies, Inc.; Rockford, IL) containing protease inhibitors and EDTA. The homogenates were centrifuged at 9600 ×*g* for 5 min to pellet the cell/tissue debris. The supernatants were carefully recovered, without disturbing the pellet, and transferred to new 1.5 mL centrifuge tubes. The supernatants were stored at − 20 °C until protein concentrations were determined. For long-term storage, the protein extracts were stored at − 75 °C.

2.6. Protein estimation

On the day of protein estimation (usually the following day after supernatants were prepared), the samples were allowed to thaw on ice and vortexed. Total protein in the supernatant was determined according to the micro-bicinchoninic acid method (Micro BCA™ Protein Assay Kit, Thermo Fisher Scientific, Waltham, MA) using bovine serum albumin as a standard.

2.7. Detection of protein expression changes in brain tissue by western immunoblotting

Aliquots of brain homogenates (6 μg total protein) diluted 1:1 in 2× Laemmli sample buffer were boiled and loaded onto 10% SDS-polyacrylamide gels. Proteins then were electrophoretically resolved and transferred to 0.45 μm Immobilon-FL polyvinylidene fluoride membranes (cat# IPFL00010, Millipore; Billerica, MA). Following transfer, immunoblot analysis was performed. Briefly, membranes were blocked using Odyssey Blocking Buffer (cat# P/N: 927–70,001, LI-COR Biosciences; Lincoln, NE) for 1 h at room temperature, washed (1 × 5 min; 2 × 10 min) with phosphate-buffered saline containing TWEEN® 20 (PBST), and incubated overnight at 4 °C with the primary antibodies (30–50 ng/mL primary antibody buffer) to synaptophysin 1 (SYP; cat# sc-17,750, mouse monoclonal, Santa Cruz Biotechnology, Inc.; Santa Cruz, CA; 35 kDa), synaptotagmin 1 (SYT; cat# sc-393,392, mouse monoclonal, Santa Cruz Biotechnology, Inc.; 60 kDa), tyrosine 3-monooxygenase/tryptophan 5-monooxygenase activation protein epsilon (YWHAE or 14–3–3ε; cat# sc-23,957, mouse monoclonal, Santa Cruz Biotechnology, Inc.; 28 kDa), glial fibrillary acidic protein (GFAP; cat# Z0334, rabbit polyclonal, DAKO North America Inc.; Carpinteria, CA; 50 kDa), tyrosine hydroxylase (TH; cat# AB9983, rabbit polyclonal, Millipore, Temecula, CA or cat# LNC1-P, mouse monoclonal, AVES Labs, Davis, CA; 56 kDa), PARK5 (UCHL1/PGP 9.5; cat# U5258, rabbit polyclonal, Sigma-Aldrich, St. Louis, MO; 26 kDa), and PARK7 (DJ1; cat# NB100–1194, goat polyclonal, Novus Biologicals, Centennial, CO; 22 kDa). β-Actin (ACTB; cat# sc-47,778, mouse monoclonal, Santa Cruz Biotechnology, Inc.; 46 kDa) was used as endogenous control. Primary antibodies procured from Santa Cruz Biotechnology were pre-conjugated with AF680 or AF790 near-infrared fluorescent dyes and used directly without the need

for IRDye-conjugated secondary antibody incubations. Following incubation with other primary antibodies, the blots were washed with PBST (1 × 5 min; 3 × 10 min) and then incubated for 1 h at room temperature with appropriate secondary antibodies conjugated with near-infrared fluorescent dyes, IRDye 680 or IRDye 800 (LI-COR Biosciences; Lincoln, NE). The membranes were protected from light to minimize any photo-bleaching of the fluorescent dyes. Membranes were washed (1 × 5 min; 4 × 10 min) in PBST, followed by washes (2 × 3 min) in PBS. Near-infrared fluorescence detection was performed using the Odyssey Imaging System (LI-COR Biosciences). The fluorescent signal intensities (*k* counts) of the individual bands were determined and normalized to ACTB. There were no differences in the basal protein expression (control) levels within a region among the different exposure regimens. However, protein expression levels varied between regions and this is to be expected given the cellular heterogeneity of the brain areas. The data are graphically represented as percent of air-exposed controls to depict increases or decreases in protein expression.

2.8. Statistical analysis

Due to the type and design of the atomizer system for vapor generation, as well as the inhalation chamber, COV exposures for acute and sub-chronic regimens were conducted independently. Each exposure had a control (HEPA-filtered air) group associated with it, and was utilized to calculate percent change from the control group for each variable. The statistical analysis incorporated both dose and days post-exposure by running two-way ANOVAs for each independent variable. Post-hoc comparisons between treatment groups at each time were generated using Fishers LSD. The data analysis reported in this paper was generated using SAS/STAT software Version 9 for the SAS System for Windows. Exploratory data analysis was performed using JMP software Version 13.

Graphical representations are means ± SEM. Results were considered significant at $P < 0.05$. *Is indicative of significant increase from the corresponding air-exposed control. #Is indicative of significant decrease from the corresponding air-exposed control.

3. Results

3.1. COV causes brain-region specific changes in biogenic amine neurotransmitters

Neurotransmitters are endogenous chemicals that play an important role in neuronal communication and maintenance of brain function. Dysregulation or imbalance of the physiological levels of neurotransmitters is associated with neurological conditions like schizophrenia, depression, mood disorders, and neurodegenerative disorders like Parkinson's disease (PD) and Alzheimer's disease (AD). Neurotoxicants, metals, particulate matter, mineral dusts, and oil dispersants have been shown to affect various neurotransmitter systems, such as adrenergic, dopaminergic, serotonergic, cholinergic and GABAergic (Sriram et al., 2004, 2011, 2012, 2014; Tin-Tin-Win-Shwe et al., 2008; Allen et al., 2014). To determine if exposure to COV exposure similarly affects neurotransmitters in the brain, we specifically examined changes in the biogenic amine neurotransmitters, NE, EPI, DA, 5-HT, DOPAC, HVA, and 5-HIAA using HPLC-EC.

Acute COV exposure did not alter NE levels in OB, STR or MB at all time points examined (Fig. 1A), although a small but non-significant reduction in NE (16% decrease) was seen in the OB (Fig. 1A), 28 d after exposure.

Acute COV exposure also caused a small, but non-significant reduction in EPI (25% decrease) in the OB 1 d after exposure (Fig. 1B). However, by 28 d post-exposure, EPI levels significantly increased (46%) above control levels (Fig. 1B). In the STR, an increase in EPI (35%) was seen at 1 d, but by 28 d a small reduction in EPI (16% decrease) was observed (Fig. 1B). In the MB, a small decrement in EPI (20% decrease) was seen 1 d after acute COV exposure, but by 28 d, EPI levels increased (37%) above control levels (Fig. 1B).

Acute COV exposure did not alter DA levels in the OB, STR and MB at all time points examined (Fig. 2A).

Following acute COV exposure, 5-HT levels were unaltered in the OB and STR at all time points examined (Fig. 2B). However, a significant increase in 5-HT (42%) was seen in the MB, 1 d after acute COV exposure (Fig. 2B), and a concurrent increase in its metabolite 5-HIAA (57%) was also seen at this time point (Table ST2). However, the 5-HIAA/5-HT ratio was not significantly altered (Table ST3).

Sub-chronic COV exposure caused significant reductions in NE levels in the STR (36% decrease) and MB (23% decrease) after 90 d (Fig. 3A). NE level remained unchanged in the OB at all the time points examined (Fig. 3A).

A robust increase in EPI level (337%) was seen in the OB 90 d after sub-chronic COV exposure but not at the earlier time points (Fig. 3B). On the other hand, significant reductions in EPI occurred in the STR (51% decrease) and MB (51% decrease) after 90 d but not at the earlier time points (Fig. 3B).

DA levels were unaltered in the OB and STR (Fig. 4A), at all the time points examined, after sub-chronic COV exposure. However, a reduction in DOPAC (37% decrease; Table ST5) and DOPAC/DA ratio (30% decrease; Table ST6) was seen in the OB, 90 d after COV exposure. In the MB, a significant reduction in DA (37% decrease) was seen after 90 d, but not at the earlier time points (Fig. 4A), and a concurrent reduction in its metabolites, DOPAC (26% decrease), and HVA (30% decrease) were also observed at this time point (Table ST5).

5-HT levels were significantly increased in the OB (62%) and STR (232%), 90 d after sub-chronic COV exposure, but not at the earlier time points (Fig. 4B). In contrast, significant reductions in 5-HIAA (39% decrease; Table ST5), and 5-HIAA/5-HT ratio (50% decrease; Table ST6) was seen in the OB, 90 d after COV exposure. Concurrent with the increase in 5-HT in the STR, a robust increase in 5-HIAA (583%; Table ST5) was observed 90 d after COV exposure. 5-HT levels remained unchanged in the MB at all the time points examined, after sub-chronic COV exposure (Fig. 4B). However, a large reduction in 5-HIAA (73% decrease; Table ST5) was seen in the MB, 90 d after COV exposure, but the 5-HIAA/5-HT ratio was not significantly altered (Table ST6).

3.2. COV causes brain-region specific changes in the expression of neuronal synaptic proteins

Chemical synaptic transmission occurs primarily through the release of neurotransmitters at the synapse. Since both acute and sub-chronic COV exposure differentially altered biogenic amine neurotransmitters in the OB, STR and MB, we examined whether COV also affected neuronal synaptic proteins, given their intrinsic involvement in the release, transport and regulation of neurotransmitters. Specifically, we evaluated changes in SYP, a major integral membrane protein of synaptic vesicles and a key presynaptic marker; SYT, a major isoform of synaptotagmin in the brain and a critical calcium-sensor associated with neurotransmitter release; and YWHAE, a synaptic membrane protein that is involved in regulating short- and long-term synaptic plasticity and neuronal migration. The expression levels of these proteins were determined by western immunoblot analysis.

Following acute COV exposure, SYP and SYT protein levels remained unaffected in all brain regions examined (OB, STR, MB) at 28 d post-exposure (Fig. 5). However, a significant increase in YWHAE protein (45%) level was seen in the MB after 28 d (Fig. 5), but not in OB or STR (Fig. 5). Immunoblot images from which the data were obtained are shown in Figs. S1, S2, and S3.

Following sub-chronic COV exposure, a significant increase in SYP protein was seen in the OB (44.5%) 1 d post-exposure but not at other time points examined (Fig. 6A). In the STR, increased SYP protein (57%) levels were seen only at 90 d, while in the MB, SYP protein increased at 28 d (49%) and 90 d (35%) after exposure (Fig. 6A). Immunoblot images from which the data were obtained are shown in Figs. S4A, S5A, and S6A.

Similarly, sub-chronic COV exposure caused a significant increase of SYT protein in the OB at 1 d (76%) and 28 d (31%) post-exposure (Fig. 6B). In the STR, increased SYT protein (50%) was seen only at 90 d (Fig. 6B), while in the MB, SYT protein increased at all time points examined, *i.e.*, at 1 d (31%), 28 d (31%) and 90 d (45%; Fig. 6B). Immunoblot images from which the data were obtained are shown in Figs. S4B, S5B, and S6B.

Sub-chronic COV exposure, did not alter YWHAE protein in the OB and STR at all time points examined (Fig. 6C). A significant increase in YWHAE protein was seen in the MB at 28 d (57%) post-exposure (Fig. 6C), but returned to baseline levels by 90 d (Fig. 6C). Immunoblot images from which the data were obtained are shown in Figs. S4C, S5C, and S6C.

3.3. COV causes brain-region specific changes in the expression of markers associated with dopaminergic neurotoxicity

TH is the rate-limiting enzyme in the synthesis of the neurotransmitter DA. Modulation of its function or loss of TH protein is an index of dopaminergic injury. Parkinson's disease-related (PARK) genes are normally involved in affording neuroprotection against oxidative stress resulting from mitochondrial dysfunction. In humans, loss-of-function mutations in PARK genes are associated with early-onset Parkinsonism. We therefore examined the expression of TH, PARK5 and PARK7 proteins to see if COV exposure causes dopaminergic deficits.

Acute exposure to COV caused a significant increase in TH protein (37%) level in the MB (Fig. 7) 28 d after exposure, but not in OB or STR (Fig. 7). Acute exposure to COV caused significant reductions in PARK5 (22% decrease) and PARK 7 (31% decrease) proteins in the OB (Fig. 7) 28 d after exposure. PARK5 protein level was unaffected in the STR and MB (Fig. 7), 28 d after exposure. On the other hand, a significant increase in PARK7 protein was seen in the STR (33%) and MB (52%), 28 d post-exposure (Fig. 7). Immunoblot images from which the data were obtained are shown in Figs. S1, S2, and S3.

Sub-chronic COV exposure, caused a significant increase of TH protein levels in the OB (42%) at 1 d post-exposure, but not at other time points examined (Fig. 8A). Sub-chronic COV exposure did not alter TH protein in the STR or MB at all time points examined (Fig. 8A). Immunoblot images from which the data were obtained are shown in Figs. S4D, S5D, and S6D.

Sub-chronic COV exposure did not alter PARK5 protein levels in the OB (Fig. 8B). In the STR, an initial reduction in PARK5 protein was seen at 1 d (34% decrease) post-exposure followed by upregulated protein expression at 28 d (42%) and 90 d (53%) post-exposure (Fig. 8B). Sub-chronic COV exposure also increased PARK5 protein in the MB at 28 d post-exposure, but not at other time points examined (Fig. 8B). Immunoblot images from which the data were obtained are shown in Figs. S4E, S5E, and S6E.

Sub-chronic COV exposure, caused a significant increase in PARK7 protein in the OB (41%) at 1 d post-exposure, but not at subsequent time points examined (Fig. 8C). PARK7 protein expression was unaffected in the STR at all time points examined (Fig. 8C). A significant increase in PARK7 protein was seen at 1 d (57%) and 28 d (69%) post-exposure in the MB (Fig. 8C) that recovered to baseline levels by 90 d post-exposure (Fig. 8C). Immunoblot images from which the data were obtained are shown in Figs. S4F, S5F, and S6F.

3.4. Changes in GFAP protein expression following COV exposure

Reactive astrogliosis is a ubiquitous feature of neuronal injury and the astrocyte marker, GFAP, is known to be altered by a variety of brain insults (Sriram et al., 2004; O'Callaghan and Sriram, 2005).

Acute exposure to COV caused a significant increase in GFAP protein (41%) levels in the MB (Fig. 9A) 28 d after exposure, but not in OB or STR (Fig. 9A). Immunoblot images from which the data were obtained are shown in Figs. S1, S2, and S3.

Sub-chronic COV exposure, caused a significant increase in GFAP protein in the OB (98%) at 1 d post-exposure, but not at the subsequent time points examined (Fig. 9B). GFAP protein expression was unaffected in the STR at all time points examined (Fig. 9B). Increased GFAP protein was also seen in the MB at 1 d (32%) and 28 d (56%) after sub-chronic COV exposure but was not statistically significant (Fig. 9B). Immunoblot images from which the data were obtained are shown in Figs. S4G, S5G, S6G.

4. Discussion

Worker exposure to COV can occur during drilling, transportation, storage, as well as fractionation and refining (Verma et al., 2000; Esswein et al., 2014; Harrison et al., 2016; Retzer et al., 2018). Additionally, worker and human exposures can occur during accidental oil spills (D'Andrea and Reddy, 2018). HHE surveys, conducted by NIOSH, identified a variety of neurological symptoms among the DWH cleanup workers (King and Gibbins, 2011). However, as a significant number of response workers who experienced neurological symptoms were exposed to both crude oil and the oil dispersant that was aerially sprayed to the contain the spill, the health effects of COV exposures alone required investigation, especially in the face of the limited toxicological information available on COV. In continuation of the efforts to characterize the toxic potential of other chemical hazards encountered by the DWH oil spill response workers, as well as workers in the oil and gas industry, in general, the present study evaluated the neurotoxic risks of exposure to COV.

Crude oil is a complex mixture of organic chemicals, metals, salts and gases (IARC, 1989; Lin and Tjeerdema, 2008; Downey, 2009). The composition of the crude oil is influenced by the geographical region, the oil field location, and the depth in the upper strata of the earth's crust from which the oil is extracted (IARC, 1989; Downey, 2009). It is mainly composed of hydrocarbons (alkanes, cycloalkanes/naphthenes, and aromatics) that vary from 50% to 97% depending on the source of the oil, and small amounts of non-hydrocarbons (like asphaltenes, resins, metal–porphyrin complexes, and trace elements). Among the alkanes found in the crude oil are methane, ethane, propane, butane, hexane, heptane, octane, and nonane. Cycloalkanes (cycloparaffins or naphthenes) like cyclopentanes and cyclohexanes make up 30–60% of the crude oil. The aromatic hydrocarbons contained in crude oil include, benzene, benzene derivatives (alkylbenzenes like toluene, xylenes, ethylbenzene), and fused-benzene ring compounds/polycyclic aromatic hydrocarbons (pyrene, fluoranthene, anthracene, chrysene, benzopyrene; IARC, 1989). BTEX are some of the naturally occurring VOC in crude oil. BTEX levels are good indicators of VOC emissions and can be periodically or continuously monitored during processing and handling of crude oil, crude distillates or industrial emissions (US EPA, 1994; ATSDR, 2004).

Inhaled COV can potentially permeate or translocate to the brain *via* olfactory or systemic circulation, thereby eliciting nervous system abnormalities. Hydrocarbons in the COV can cause perturbation of cellular membranes. Specifically, lipophilic hydrocarbons can accumulate in the membrane lipid bilayer and alter the lipid-protein structure, thereby affecting the permeability, integrity, and function of the membrane (Sikkema et al., 1995), including intracellular signaling. Indeed, exposure to hydrocarbons typically seen in crude oil, such as benzene, toluene, and xylene, have been shown cause neurological symptoms like headache, dizziness, numbness and tingling sensation, blurred or double vision, confusion, decreased ability to focus, memory loss, and unconsciousness or fainting (Burbacher, 1993; Benignus et al., 2007; Bahadar et al., 2014; Niaz et al., 2015). A few studies have also investigated the association between oil spills and neurological symptoms among oil spill response workers and residents near oil spill areas. Symptoms such as, headache, dizziness, and memory loss have been reported (Lyons et al., 1999; Morita et al.,

1999; Carrasco et al., 2006; Ha et al., 2008; Cheong et al., 2011; Na et al., 2012; Peres et al., 2016).

We hypothesized that the alkanes, cycloalkanes/naphthenes, and aromatic hydrocarbons present in COV may affect neuronal membranes causing aberrant synaptic signaling and impaired neurotransmission, defects that can culminate in neural damage. To examine this, we evaluated changes in biogenic amine neurotransmitters and expression of neural markers, including synaptic and PD-related proteins. Acute exposure to COV resulted in a decrease in NE levels and an increase in EPI levels in the OB, while the sub-chronic COV exposure increased EPI and 5-HT levels in the OB, suggesting an imbalance in the levels of these neurotransmitters. Monoamines like DA, NE, EPI, and 5-HT have been shown to modulate olfactory function, including odor processing and odor discrimination (Rosser and Keverne, 1985; Gray et al., 1986; Escanilla et al., 2010). Specifically, NE is known to modulate odor habituation (Guerin et al., 2008), while 5-HT regulates odor inputs (Petzold et al., 2009) in the OB. Sub-chronic COV exposure also caused an early increase in the protein levels of SYP and SYT in the OB. SYP and SYT are involved in synaptic transmission and their increased expression, as observed here, may be associated with long-term potentiation of synaptic mechanisms for altering neurotransmitter release and olfactory memory formation. Olfactory sensory neurons make up a large portion of the olfactory epithelium, and thus odorant molecules, chemicals, metals, allergens, pollutants, and microorganisms can potentially gain entry through retrograde axonal transport across the olfactory neurons (Doty, 2015). Some of these toxicants can be potentially harmful, causing olfactory sensory deafferentation. Although these neurons have the unique ability to regenerate throughout the lifespan of an animal (Crews and Hunter, 1994), repeated exposure to toxicants can render an irreversible injury resulting in reduction or loss of olfactory function. Indeed, hyposmia or anosmia are non-motor symptoms associated with neurodegenerative disorders, including PD, a movement disorder primarily involving the dopaminergic neuron pathway (Baba et al., 2011; Ruan et al., 2012; Attems et al., 2014). However, olfactory or neurobehavioral assessments were not conducted in this initial hazard identification study; thus, the functional relevance of such molecular changes cannot be proven conclusively. Nevertheless, these early molecular events are suggestive of neural abnormality following COV exposure. Additional long-term studies are necessary to determine if such changes contribute to olfactory deficits and neurodegenerative pathology.

In the dopaminergic brain regions, STR and MB, sub-chronic COV exposure caused a delayed reduction in NE, EPI, and DA content. The striatum, nucleus accumbens, and midbrain are enriched with alpha- and beta-adrenergic receptors (Nicholas et al., 1993; Pisani et al., 2003; Paschalis et al., 2009; Rommelfanger et al., 2009), which are primarily expressed on presynaptic terminals and post-synaptic terminals and cell bodies (Pisani et al., 2003; Paschalis et al., 2009; Rommelfanger et al., 2009; Hara et al., 2010; Meitzen et al., 2011), suggesting an important role for NE in striatal signaling. Dysregulation of NE in the striatum has been linked to dopaminergic neurotoxicity, as well as PD (Fornai et al., 1997; Fornai et al., 2007; Rommelfanger et al., 2007; Rommelfanger and Weinshenker, 2007). These findings suggest that modulation NE-mediated neurotransmission can alter striatal signaling and consequently elicit functional outcomes, including affording neuroprotection by regulating striatal control of motor function (Marien et al., 2004; Rommelfanger and

Weinshenker, 2007). The robust increase in NE in the striatum seen following COV exposure is likely linked to its neuroprotective role, and is consistent with the increased expression of PARK-related proteins, PARK5 and PARK7, seen after COV exposure.

Consistent with this, COV also augmented the expression of several synaptic complex proteins associated with neurotransmission in these two brain regions. Specifically, increased expression of SYP, SYT, and YWHAE occurred. Such abnormal accumulation of presynaptic proteins can result in functional disturbances. Undeniably, these changes are consistent with that observed in the OB and are indicative of their involvement in modulating neurotransmitter release and dopaminergic function. SYP and SYT are major synaptic vesicle protein involved in vesicle sorting, priming, synaptic biogenesis, synapse formation, exocytosis, and endocytosis. SYP is a reliable marker of axonal damage (Gudi et al., 2017) and SYT plays a key role in axonal neurotransmitter release, including release of DA (Mendez et al., 2011; Banerjee et al., 2020). Impairment of axonal transport and/or axonal damage are notable features of neuroinflammatory and neurodegenerative diseases, like PD, AD, and multiple sclerosis (De Vos et al., 2008; Millecamps and Julien, 2013; Gudi et al., 2017). Indeed, studies have reported that dynamic changes in the expression of presynaptic and axonal proteins precedes dopaminergic neurotoxicity (Chung et al., 2009), findings consistent with our observations.

Besides increasing synaptic proteins in these dopaminergic brain regions, sub-chronic COV exposure also caused a concordant increase in PARK5 and PARK7 proteins in these brain regions. PARK5 (UCHL1), a deubiquitinating enzyme that is highly expressed in the brain (Day and Thompson, 1987), is an important component of the ubiquitin proteosome pathway (UPP). The UPP is essential for removing abnormal proteins and, thereby, preventing unwanted buildup of potentially toxic proteins in the neurons (Graham and Liu, 2017; Liu et al., 2019). Dysfunction of UPP, as seen in aging, is linked to abnormal accumulation of protein aggregates within neurons in neurodegenerative disorders like PD and AD (Graham and Liu, 2017; Liu et al., 2019). UCHL1 (PARK5 gene) deletion has been linked to axonal degeneration, sensory ataxia, and premature death in mice (Mi et al., 2021). PARK5 is also known to play a role in the pathogenesis of neurodegenerative diseases and recovery after neuronal injury (Mi et al., 2021). PARK5 is involved in tagging over-expressed or damaged proteins with ubiquitin for subsequent degradation by the proteasome. Additionally, PARK5 also exhibits a hydrolase activity whereby it deubiquitinates proteins and recycles the ubiquitin to sustain the protein degradation pathway (Bishop et al., 2016). Like PARK5, PARK7 (DJ1) has been shown to be expressed in the brain, including in neurons within the substantia nigra pars compacta and STR, areas primarily affected in PD (Olzmann et al., 2007). PARK7 mutations account for about 1–2% of early-onset cases of PD (Hague et al., 2003; Hedrich et al., 2004). Mice deficient in PARK7 exhibit exacerbated nigrostriatal neurodegeneration after treatment with the dopaminergic neurotoxicant, MPTP (Kim et al., 2005). Disruption of PARK7 also causes nigrostriatal dopaminergic deficits, hypokinesia and alterations in dopamine D2 receptor-related functions in the substantia nigra, located within the MB (Goldberg et al., 2005). PARK7 expression has been localized to the matrix and inter-membrane space of mitochondria (Canet-Aviles et al., 2004; Zhang et al., 2005) and is thought to function as an anti-oxidant protein (Taira et al., 2004). PARK7 knockout mice exhibit increased mitochondrial free radical production and inactivated

mitochondrial enzymes (Andres-Mateos et al., 2007). Down-regulation of PARK7 gene is linked to enhanced cell death through exacerbation of oxidative stress and proteasome inhibition (Yokota et al., 2003). With this understanding of the functional roles of PARK5 and PARK7, the increased expression of these two proteins in the STR and MB following COV exposure perhaps reflects a protective mechanism to clear over-expressed or defective/abnormal proteins, control oxidant damage, and maintain mitochondrial integrity.

In humans, mood disorders are often associated with altered activity in neural circuits involving various brain regions, including STR (Konarski et al., 2006; Ressler and Mayberg, 2007; Krishnan and Nestler, 2010; Marchand and Yurgelun-Todd, 2010). Deficit or imbalance in the central monoaminergic neurotransmitters is thought to be involved in mood disorders (Tissot, 1975; Syvalahti, 1987). Specifically, NE and 5-HT play a role in depression and anxiety disorder. The alterations in monoamine neurotransmitters and synaptic proteins elicited by COV are suggestive of abnormal neurotransmission. HHE surveys, conducted by NIOSH, among DWH oil-spill response workers identified that about 16 % of workers employed in decontamination and waste management operations, reported one or more psychosocial symptoms that included depressed feeling, worries, stress, short temper and frequent alterations in mood (King and Gibbins, 2011). Unfortunately, whether such health effects were caused by exposure to crude oil or oil dispersant has been difficult to discern, as exposure to both agents is likely to have occurred. Whether, the neurochemical and synaptic changes elicited by COV are the underpinnings of the psychosocial symptoms reported by the oil-spill response workers, remains to be investigated.

While we have no direct evidence to demonstrate the presence of COV components in the brain, it is likely that membrane permeation or systemic translocation of the hydrocarbons in COV through the olfactory or pulmonary targets may be the underlying basis for the observed neuronal abnormalities. Alternatively, stimulation or deafferentation of the olfactory sensory neurons may itself suffice to cause perturbations in other brain areas.

Collectively, our findings suggest that an imbalance in monoaminergic signaling, as a consequence of synaptic modulation, may underlie the neurotoxicity associated with COV exposure. It is possible that such alterations in neurotransmitter signaling can contribute to functional neurological abnormalities like depression, lack of coordination and short-term memory loss. The specific involvement of the dopaminergic brain areas, STR and MB, and the altered expression of PARK proteins are further indicative of perturbations in the dopaminergic pathway associated with movement disorders like PD. Such functional deficits were not observed in this preliminary hazard identification study; nevertheless, our findings call for further evaluation of the neurotoxic potential of COV, including comprehensive assessments of long-term neurochemical, neurodegenerative, and neurobehavioral outcomes.

Supplementary Material

Refer to Web version on PubMed Central for supplementary material.

Acknowledgements

Funding was provided by the National Institute for Occupational Safety and Health, Project Number 7927ZLDC.

References

Allen JL, Liu X, Pelkowski S, Palmer B, Conrad K, Oberdorster G, Weston D, Mayer-Proschel M, Cory-Slechta DA, 2014. Early postnatal exposure to ultrafine particulate matter air pollution: persistent ventriculomegaly, neurochemical disruption, and glial activation preferentially in male mice. Environ. Health Perspect. 122, 939–945. [PubMed: 24901756]

Andres-Mateos E, Perier C, Zhang L, Blanchard-Fillion B, Greco TM, Thomas B, Ko HS, Sasaki M, Ischiropoulos H, Przedborski S, Dawson TM, Dawson VL, 2007. DJ-1 gene deletion reveals that DJ-1 is an atypical peroxiredoxin-like peroxidase. Proc. Natl. Acad. Sci. U. S. A. 104, 14807–14812. [PubMed: 17766438]

ATSDR, 2004. Interaction Profile for: Benzene, Toluene, Ethylbenzene, and Xylenes (BTEX). U.S. Department of Health and Human Services, Agency for Toxic Substances and Disease Registry. https://www.atsdr.cdc.gov/interactionprofiles/ip-btex/ip05.pdf (Accessed January 19, 2022).

Attems J, Walker L, Jellinger KA, 2014. Olfactory bulb involvement in neurodegenerative diseases. Acta Neuropathol. 127, 459–475. [PubMed: 24554308]

Baba T, Takeda A, Kikuchi A, Nishio Y, Hosokai Y, Hirayama K, Hasegawa T, Sugeno N, Suzuki K, Mori E, Takahashi S, Fukuda H, Itoyama Y, 2011. Association of olfactory dysfunction and brain. Metabolism in Parkinson's disease. Mov. Disord. 26, 621–628. [PubMed: 21284041]

Bahadar H, Mostafalou S, Abdollahi M, 2014. Current understandings and perspectives on non-cancer health effects of benzene: a global concern. Toxicol. Appl. Pharmacol. 276, 83–94. [PubMed: 24589379]

Banerjee A, Lee J, Nemcova P, Liu C, Kaeser PS, 2020. Synaptotagmin-1 is the Ca^{2+} sensor for fast striatal dopamine release. eLife 9, e58359. 10.7554/eLife.58359.

Benignus VA, Boyes WK, Kenyon EM, Bushnell PJ, 2007. Quantitative comparisons of the acute neurotoxicity of toluene in rats and humans. Toxicol. Sci. 100, 146–155. [PubMed: 17698514]

Bishop P, Rocca D, Henley JM, 2016. Ubiquitin C-terminal hydrolase L1 (UCH-L1): structure, distribution and roles in brain function and dysfunction. Biochem. J. 473, 2453–2462. [PubMed: 27515257]

Burbacher TM, 1993. Neurotoxic effects of gasoline and gasoline constituents. Environ. Health Perspect. 101 (Suppl. 6), 133–141. [PubMed: 8020437]

Canet-Aviles RM, Wilson MA, Miller DW, Ahmad R, McLendon C, Bandyopadhyay S, Baptista MJ, Ringe D, Petsko GA, Cookson MR, 2004. The Parkinson's disease protein DJ-1 is neuroprotective due to cysteine-sulfinic acid-driven mitochondrial localization. Proc. Natl. Acad. Sci. U. S. A. 101, 9103–9108. [PubMed: 15181200]

Carrasco JM, Lope V, Perez-Gomez B, Aragones N, Suarez B, Lopez-Abente G, Rodriguez-Artalejo F, Pollan M, 2006. Association between health information, use of protective devices and occurrence of acute health problems in the Prestige oil spill clean-up in Asturias and Cantabria (Spain): a cross-sectional study. BMC Public Health 6, 1. [PubMed: 16390547]

Cheong HK, Ha M, Lee JS, Kwon H, Ha EH, Hong YC, Choi Y, Jeong WC, Hur J, Lee SM, Kim EJ, Im H, 2011. Hebei spirit oil spill exposure and subjective symptoms in residents participating in clean-up activities. Environ. Health Toxicol. 26, e2011007.

Chung CY, Koprich JB, Siddiqi H, Isacson O, 2009. Dynamic changes in presynaptic and axonal transport proteins combined with striatal neuroinflammation precede dopaminergic neuronal loss in a rat model of AAV alpha-synucleinopathy. J. Neurosci. 29, 3365–3373. [PubMed: 19295143]

Crews L, Hunter D, 1994. Neurogenesis in the olfactory epithelium. Perspect. Dev. Neurobiol. 2, 151–161. [PubMed: 7728499]

D'Andrea MA, Reddy GK, 2018. The development of long-term adverse health effects in oil spill cleanup workers of the deepwater horizon offshore drilling rig disaster. Front. Public Health 6, 117. [PubMed: 29755965]

Day IN, Thompson RJ, 1987. Molecular cloning of cDNA coding for human PGP 9.5 protein. A novel cytoplasmic marker for neurones and neuroendocrine cells. FEBS Lett. 210, 157–160. [PubMed: 2947814]

De Vos KJ, Grierson AJ, Ackerley S, Miller CC, 2008. Role of axonal transport in neurodegenerative diseases. Ann. Rev. Neurosci. 31, 151–173. 10.1146/annurev.neuro.31.061307.090711. [PubMed: 18558852]

Divine Barbara J., Barron Virginia, 1987. Texaco mortality study: III. A cohort study of producing and pipeline workers. Am. J. Ind. Med. 11, 189–202. 10.1002/ajim.4700110208. [PubMed: 3826079]

Divine BJ, Hartman CM, 2000. Update of a study of crude oil production workers 1946–94. Occup. Environ. Med. 57, 411–417. [PubMed: 10810131]

Doherty BT, Kwok RK, Curry MD, Ekenga C, Chambers D, Sandler DP, Engel LS, 2017. Associations between blood BTEXS concentrations and hematologic parameters among adult residents of the U.S. Gulf States. Environ. Res. 156, 579–587. [PubMed: 28448810]

Doty RL, 2015. Neurotoxic exposure and impairment of the chemical senses of taste and smell. Handb. Clin. Neurol. 131, 299–324. [PubMed: 26563795]

Downey M, 2009. Oil 101. Wooden Table Press, New York, NY.

EPA, U.S., 1994. An evaluation of four field screening techniques for measurement of BTEX. U.S. Environmental Protection Agency. EPA 600/R-94/181. https://nepis.epa.gov/Exe/ZyPDF.cgi?Dockey=94002YOO.PDF (Accessed January 19, 2022).

Escanilla O, Arrellanos A, Karnow A, Ennis M, Linster C, 2010. Noradrenergic modulation of behavioral odor detection and discrimination thresholds in the olfactory bulb. Eur. J. Neurosci. 32, 458–468. [PubMed: 20618829]

Esswein EJ, Snawder J, King B, Breitenstein M, Alexander-Scott M, Kiefer M, 2014. Evaluation of some potential chemical exposure risks during flowback operations in unconventional oil and gas extraction: preliminary results. J. Occup. Environ. Hyg. 11, D174–D184. [PubMed: 25175286]

Fedan JS, 2022. Biological effects of inhaled crude oil vapor. I. Scope of the investigation. Toxicol. Appl. Pharmacol. In this issue.

Fedan JS, Thompson JA, Russ KA, Dey RD, Reynolds JS, Kashon ML, Jackson MC, McKinney W, 2022. Biological effects of inhaled crude oil vapor. II. Pulmonary effects. Toxicol. Appl. Pharmacol. In this issue.

Fornai F, Bassi L, Bonaccorsi I, Giorgi F, Corsini GU, 1997. Noradrenaline loss selectivity exacerbates nigrostriatal toxicity in different species of rodents. Funct. Neurol. 12, 193–198. [PubMed: 9218976]

Fornai F, di Poggio AB, Pellegrini A, Ruggieri S, Paparelli A, 2007. Noradrenaline in Parkinson's disease: from disease progression to current therapeutics. Curr. Med. Chem. 14, 2330–2334. [PubMed: 17896981]

Goldberg MS, Pisani A, Haburcak M, Vortherms TA, Kitada T, Costa C, Tong Y, Martella G, Tscherter A, Martins A, Bernardi G, Roth BL, Pothos EN, Calabresi P, Shen J, 2005. Nigrostriatal dopaminergic deficits and hypokinesia caused by inactivation of the familial parkinsonism-linked gene DJ-1. Neuron. 45, 489–496. [PubMed: 15721235]

Graham SH, Liu H, 2017. Life and death in the trash heap: the ubiquitin proteasome pathway and UCHL1 in brain aging, neurodegenerative disease and cerebral ischemia. Ageing Res. Rev. 34, 30–38. [PubMed: 27702698]

Gray CM, Freeman WJ, Skinner JE, 1986. Chemical dependencies of learning in the rabbit olfactory bulb: acquisition of the transient spatial pattern change depends on norepinephrine. Behav. Neurosci. 100, 585–596. [PubMed: 3017376]

Gudi V, Gai L, Herder V, Tejedor LS, Kipp M, Amor S, Suhs KW, Hansmann F, Beineke A, Baumgartner W, Stangel M, Skripuletz T, 2017. Synaptophysin is a reliable marker for axonal damage. J. Neuropathol. Exp. Neurol. 76, 109–125. [PubMed: 28177496]

Guerin D, Peace ST, Didier A, Linster C, Cleland TA, 2008. Noradrenergic neuromodulation in the olfactory bulb modulates odor habituation and spontaneous discrimination. Behav. Neurosci. 122, 816–826. [PubMed: 18729635]

Ha M, Lee WJ, Lee S, Cheong HK, 2008. A literature review on health effects of exposure to oil spill. J. Prev. Med. Public Health 41, 345–354. [PubMed: 18827503]

Hague S, Rogaeva E, Hernandez D, Gulick C, Singleton A, Hanson M, Johnson J, Weiser R, Gallardo M, Ravina B, Gwinn-Hardy K, Crawley A, St George-Hyslop PH, Lang AE, Heutink P, Bonifati V,

Hardy J, Singleton A, 2003. Early-onset Parkinson's disease caused by a compound heterozygous DJ-1 mutation. Ann. Neurol. 54, 271–274. [PubMed: 12891685]

Hara M, Fukui R, Hieda E, Kuroiwa M, Bateup H, Kano T, Greengard P, Nishi A, et al. , 2010. Role of adrenoceptors in the regulation of dopamine/DARPP-32 signaling in neostriatal neurons. J. Neurochem. 111 (4), 1046–1059. 10.1111/j.1471-4159.2010.06668.x.

Harrison RJ, Retzer K, Kosnett MJ, Hodgson M, Jordan T, Ridl S, Kiefer M, 2016. Sudden deaths among oil and gas extraction workers resulting from oxygen deficiency and inhalation of hydrocarbon gases and vapors - United States, January 2010-March 2015. MMWR Morb. Mortal. Wkly Rep. 65, 6–9. [PubMed: 26766558]

Hedrich K, Djarmati A, Schafer N, Hering R, Wellenbrock C, Weiss PH, Hilker R, Vieregge P, Ozelius LJ, Heutink P, Bonifati V, Schwinger E, Lang AE, Noth J, Bressman SB, Pramstaller PP, Riess O, Klein C, 2004. DJ-1 (PARK7) mutations are less frequent than Parkin (PARK2) mutations in early-onset Parkinson disease. Neurology. 62, 389–394. [PubMed: 14872018]

IARC, 1989. Occupational exposures in petroleum refining; crude oil and major petroleum fuels. IARC Working Group on the Evaluation of Carcinogenic Risks to Humans. IARC Monogr. Eval. Carcinog. Risks Hum. 45, 1–322.

Investigative Team, 2022. Biological effects of inhaled crude oil vapor. VII. Summary and conclusions. Toxicol. Appl. Pharmacol. In this issue.

Kim RH, Smith PD, Aleyasin H, Hayley S, Mount MP, Pownall S, Wakeham A, You-Ten AJ, Kalia SK, Horne P, Westaway D, Lozano AM, Anisman H, Park DS, Mak TW, 2005. Hypersensitivity of DJ-1-deficient mice to 1-methyl-4-phenyl-1,2,3,6-tetrahydropyrindine (MPTP) and oxidative stress. Proc. Natl. Acad. Sci. U. S. A. 102, 5215–5220. [PubMed: 15784737]

King BS, Gibbins JD, 2011. Health Hazard Evaluation of Deepwater Horizon Response Workers. Health Hazard Evaluation. Report HETA 2010–0115 & 2010– 0129-3138. https://www.cdc.gov/niosh/hhe/reports/pdfs/2010-0115-0129-3138.pdf (Accessed January 21, 2022).

Kirkeleit J, Riise T, Bratveit M, Moen BE, 2008. Increased risk of acute myelogenous leukemia and multiple myeloma in a historical cohort of upstream petroleum workers exposed to crude oil. Cancer Causes Control 19, 13–23. [PubMed: 17906934]

Konarski JZ, McIntyre RS, Soczynska JK, Bottas A, Kennedy SH, 2006. Clinical translation of neuroimaging research in mood disorders. Psychiatry (Edgmont) 3, 46–57.

Krajnak K, Russ KA, McKinney W, Waugh S, Zheng W, Kan W, Kashon ML, Cumpston J, Fedan JS, 2022. Biological effects of inhaled vapors from crude oil. IV. Cardiovascular effects. Toxicol. Appl. Pharmacol. In this issue.

Krishnamurthy J, Engel LS, Wang L, Schwartz EG, Christenbury K, Kondrup B, Barrett J, Rusiecki JA, 2019. Neurological symptoms associated with oil spill response exposures: results from the Deepwater Horizon Oil Spill Coast Guard Cohort Study. Environ. Int. 131, 104963.

Krishnan V, Nestler EJ, 2010. Linking molecules to mood: new insight into the biology of depression. Am. J. Psychiatry 167, 1305–1320. [PubMed: 20843874]

Lin CY, Tjeerdema RS, 2008. Crude oil, oil, gasoline and petrol. In: Jørgensen SE, Fath BD (Eds.), Encyclopedia of Ecology. Academic Press, Oxford, pp. 797–805.

Liu H, Povysheva N, Rose ME, Mi Z, Banton JS, Li W, Chen F, Reay DP, Barrionuevo G, Zhang F, Graham SH, 2019. Role of UCHL1 in axonal injury and functional recovery after cerebral ischemia. Proc. Natl. Acad. Sci. U. S. A. 116, 4643–4650. [PubMed: 30760601]

Lyons RA, Temple JM, Evans D, Fone DL, Palmer SR, 1999. Acute health effects of the sea empress oil spill. J. Epidemiol. Community Health 53, 306–310. [PubMed: 10396538]

Marchand WR, Yurgelun-Todd D, 2010. Striatal structure and function in mood disorders: a comprehensive review. Bipolar Disord. 12, 764–785. [PubMed: 21176024]

Marien MR, Colpaert FC, Rosenquist AC, 2004. Noradrenergic mechanisms in neurodegenerative diseases: a theory. Brain Res. Brain Res. Rev. 45, 38–78. [PubMed: 15063099]

McKinney W, Jackson M, Law B, Fedan J, 2022. Automated crude oil vapor inhalation exposure system. Inhal Toxicol. (In Revision) Submitted for publication.

McNutt MK, Camilli R, Crone TJ, Guthrie GD, Hsieh PA, Ryerson TB, Savas O, Shaffer F, 2012. Review of flow rate estimates of the Deepwater Horizon oil spill. Proc. Natl. Acad. Sci. U. S. A. 109, 20260–20267. [PubMed: 22187459]

Meitzen J, Luoma JI, Stern CM, Mermelstein PG, 2011. β1-Adrenergic receptors activate two distinct signaling pathways in striatal neurons. J. Neurochem. 116 (6), 984–995. 10.1111/j.1471-4159.2010.07137.x. [PubMed: 21143600]

Mendez JA, Bourque MJ, Fasano C, Kortleven C, Trudeau LE, 2011. Somatodendritic dopamine release requires synaptotagmin 4 and 7 and the participation of voltage-gated calcium channels. J. Biolo. Chem. 286 (27), 23928–23937. 10.1074/jbc.M111.218032.

Mi Z, Liu H, Rose ME, Ma X, Reay DP, Ma J, Henchir J, Dixon CE, Graham SH, 2021. Abolishing UCHL1's hydrolase activity exacerbates TBI-induced axonal injury and neuronal death in mice. Exp. Neurol. 336, 113524.

Millecamps S, Julien JP, 2013. Axonal transport deficits and neurodegenerative diseases. Nat. Rev. Neurosci. 14 (3), 161–176. 10.1038/nrn3380. [PubMed: 23361386]

Morita A, Kusaka Y, Deguchi Y, Moriuchi A, Nakanaga Y, Iki M, Miyazaki S, Kawahara K, 1999. Acute health problems among the people engaged in the cleanup of the Nakhodka oil spill. Environ. Res. 81, 185–194. [PubMed: 10585014]

Na JU, Sim MS, Jo IJ, Song HG, 2012. The duration of acute health problems in people involved with the cleanup operation of the Hebei Spirit oil spill. Mar. Pollut. Bull. 64, 1246–1251. [PubMed: 22491025]

Niaz K, Bahadar H, Maqbool F, Abdollahi M, 2015. A review of environmental and occupational exposure to xylene and its health concerns. EXCLI J. 14, 1167–1186. [PubMed: 26862322]

Nicholas AP, Pieribone V, Hokfelt T, 1993. Distributions of mRNAs for alpha-2 adrenergic receptor subtypes in rat brain: an in situ hybridization study. J. Comp. Neurol. 328, 575–594. [PubMed: 8381444]

NIOSH, 2015. Fatalities in Oil and Gas Extraction (FOG) Special Report 2015. Suspectedinhalation fatalities involving workers during manual tank gauging, sampling, and fluid transfer operations on oil and gas well sites, 2010–2014. U.S. Department of Health & Human Services, Centers for Disease Control and Prevention, National Institute for Occupational Safety and Health. https://www.cdc.gov/niosh/topics/fog/SpecialTopic2015.html#_ftn1 (Accessed January 21, 2022).

O'Callaghan JP, Sriram K, 2005. Glial fibrillary acidic protein and related glial proteins as biomarkers of neurotoxicity. Expert Opin. Drug Saf. 4, 433–442. [PubMed: 15934851]

Olzmann JA, Bordelon JR, Muly EC, Rees HD, Levey AI, Li L, Chin LS, 2007. Selective enrichment of DJ-1 protein in primate striatal neuronal processes: implications for Parkinson's disease. J. Comp. Neurol. 500, 585–599. [PubMed: 17120294]

Paschalis A, Churchill L, Marina N, Kasymov V, Gourine A, Ackland G, 2009. beta1-adrenoceptor distribution in the rat brain: an immunohistochemical study. Neurosci. Lett. 458, 84–88. [PubMed: 19442879]

Peres LC, Trapido E, Rung AL, Harrington DJ, Oral E, Fang Z, Fontham E, Peters ES, 2016. The DEEPWATER horizon oil spill and physical health among adult women in southern Louisiana: The Women and Their Children's Health (WaTCH) study. Environ. Health Perspect. 124, 1208–1213. [PubMed: 26794669]

Petzold GC, Hagiwara A, Murthy VN, 2009. Serotonergic modulation of odor input to the mammalian olfactory bulb. Nat. Neurosci. 12, 784–791. [PubMed: 19430472]

Pisani A, Bonsi P, Centonze D, Martorana A, Fusco F, Sancesario G, De Persis C, Bernardi G, Calabresi P, 2003. Activation of beta1-adrenoceptors excites striatal cholinergic interneurons through a cAMP-dependent, protein kinase-independent pathway. J. Neurosci. 23, 5272–5282. [PubMed: 12832552]

Ressler KJ, Mayberg HS, 2007. Targeting abnormal neural circuits in mood and anxiety disorders: from the laboratory to the clinic. Nat. Neurosci. 10, 1116–1124. [PubMed: 17726478]

Retzer K, Schmick E, Ramirez-Cardenas A, King B, Snawder J, 2018. Gases and vapors continue to pose hazards on oil and gas well sites during gauging, fluid transfer, and disposal. https://blogs.cdc.gov/niosh-science-blog/2018/08/24/oil-and-gas-vapors/(Accessed January 21, 2022).

Rommelfanger KS, Weinshenker D, 2007. Norepinephrine: the redheaded stepchild of Parkinson's disease. Biochem. Pharmacol. 74, 177–190. [PubMed: 17416354]

Rommelfanger KS, Edwards GL, Freeman KG, Liles LC, Miller GW, Weinshenker D, 2007. Norepinephrine loss produces more profound motor deficits than MPTP treatment in mice. Proc. Natl. Acad. Sci. U. S. A. 104, 138049.

Rommelfanger KS, Mitrano DA, Smith Y, Weinshenker D, 2009. Light and electron microscopic localization of alpha-1 adrenergic receptor immunoreactivity in the rat striatum and ventral midbrain. Neuroscience. 158, 1530–1540. [PubMed: 19068224]

Rosser AE, Keverne EB, 1985. The importance of central noradrenergic neurones in the formation of an olfactory memory in the prevention of pregnancy block. Neuroscience. 15, 1141–1147. [PubMed: 4047399]

Ruan Y, Zheng XY, Zhang HL, Zhu W, Zhu J, 2012. Olfactory dysfunctions in neurodegenerative disorders. J. Neurosci. Res. 90, 1693–1700. [PubMed: 22674288]

Rusiecki J, Alexander M, Schwartz EG, Wang L, Weems L, Barrett J, Christenbury K, Johndrow D, Funk RH, Engel LS, 2018a. The deepwater horizon oil spill coast guard cohort study. Occup. Environ. Med. 75, 165–175. [PubMed: 28899964]

Rusiecki J, Stewart P, Lee D, Alexander M, Krstev S, Silverman D, Blair A, 2018b. Mortality among Coast Guard Shipyard workers: A retrospective cohort study of specific exposures. Arch. Environ. Occup. Health 73, 4–18. [PubMed: 28166467]

Sager TM, Joseph P, Umbright CM, Hubbs AF, Barger M, Kashon ML, Fedan JS, Roberts JR, 2022. Biological effects of inhaled crude oil vapor. III. Pulmonary inflammation, cytotoxicity, and gene expression profile. Toxicol. Appl. Pharmacol. In this issue.

Sathiakumar N, Delzell E, Cole P, Brill I, Frisch J, Spivey G, 1995. A case-control study of leukemia among petroleum workers. J. Occup. Environ. Med. 37, 1269–1277. [PubMed: 8595496]

Schnatter AR, Theriault G, Katz AM, Thompson FS, Donaleski D, Murray N, 1992. A retrospective mortality study within operating segments of a petroleum company. Am. J. Ind. Med. 22, 209–229. [PubMed: 1415287]

Sikkema J, de Bont JA, Poolman B, 1995. Mechanisms of membrane toxicity of hydrocarbons. Microbiol. Rev. 59 (2), 201–222. [PubMed: 7603409]

Sriram K, Pai KS, Boyd MR, Ravindranath V, 1997. Evidence for generation of oxidative stress in brain by MPTP: in vitro and in vivo studies in mice. Brain Res. 749, 44–52. [PubMed: 9070626]

Sriram K, Shankar SK, Boyd MR, Ravindranath V, 1998. Thiol oxidation and loss of mitochondrial complex I precede excitatory amino acid-mediated neurodegeneration. J. Neurosci. 18, 10287–10296. [PubMed: 9852566]

Sriram K, Benkovic SA, Hebert MA, Miller DB, O'Callaghan JP, 2004. Induction of gp130-related cytokines and activation of JAK2/STAT3 pathway in astrocytes precedes up-regulation of glial fibrillary acidic protein in the 1-methyl-4-phenyl-1,2,3,6-tetrahydropyridine model of neurodegeneration: key signaling pathway for astrogliosis in vivo? J. Biol. Chem. 279, 19936–19947. [PubMed: 14996842]

Sriram K, Lin GX, Jefferson AM, Goldsmith WT, Jackson M, McKinney W, Frazer DG, Robinson VA, Castranova V, 2011. Neurotoxicity following acute inhalation exposure to the oil dispersant COREXIT EC9500A. J. Toxicol. Environ. Health A. 74, 1405–1418. [PubMed: 21916746]

Sriram K, Lin GX, Jefferson AM, Roberts JR, Andrews RN, Kashon ML, Antonini JM, 2012. Manganese accumulation in nail clippings as a biomarker of welding fume exposure and neurotoxicity. Toxicology. 291, 73–82. [PubMed: 22085607]

Sriram K, Jefferson AM, Lin GX, Afshari A, Zeidler-Erdely PC, Meighan TG, McKinney W, Jackson M, Cumpston A, Cumpston JL, Leonard HD, Frazer DG, Antonini JM, 2014. Neurotoxicity following acute inhalation of aerosols generated during resistance spot weld-bonding of carbon steel. Inhal. Toxicol. 26, 720–732. [PubMed: 25265048]

Sriram K, Lin GX, Jefferson AM, McKinney W, Jackson MC, Cumpston A, Cumpston JL, Cumpston JB, Leonard HD, Kashon M, Fedan JS, 2020. Biological effects of inhaled hydraulic fracturing sand dust VII. Neuroinflammation and altered synaptic protein expression. Toxicol. Appl. Pharmacol. 409 (115300).

Stenehjem JS, Kjaerheim K, Rabanal KS, Grimsrud TK, 2014. Cancer incidence among 41,000 offshore oil industry workers. Occup. Med. (Lond.) 64, 539–545. [PubMed: 25082833]

Syvalahti E, 1987. Monoaminergic mechanisms in affective disorders. La Medicina Biologica 65, 89–96.

Taira T, Saito Y, Niki T, Iguchi-Ariga SM, Takahashi K, Ariga H, 2004. DJ-1 has a role in antioxidative stress to prevent cell death. EMBO Rep. 5, 213–218. [PubMed: 14749723]

Tin-Tin-Win-Shwe Mitsushima, D., Yamamoto S, Fukushima A, Funabashi T, Kobayashi T, Fujimaki H, 2008. Changes in neurotransmitter levels and proinflammatory cytokine mRNA expressions in the mice olfactory bulb following nanoparticle exposure. Toxicol. Appl. Pharmacol. 226, 192–198. [PubMed: 17950771]

Tissot R, 1975. The common pathophysiology of monaminergic psychoses: a new hypothesis. Neuropsychobiology. 1, 243–260. [PubMed: 775359]

Valentic D, Stojanovic D, Micovic V, Vukelic M, 2005. Work related diseases and injuries on an oil rig. Int. Marit. Health. 56, 56–66. [PubMed: 16532585]

Verma DK, Johnson DM, McLean JD, 2000. Benzene and total hydrocarbon exposures in the upstream petroleum oil and gas industry. AIHAJ. 61, 255–263. [PubMed: 10782197]

Weatherly LM, Shane HL, Baur R, Lukomska E, Roberts JR, Fedan JS, Anderson SE, 2022. Biological effects of inhaled crude oil vapor. VI. Immunotoxicity. Toxicol. Appl. Pharmacol. In this issue.

Wong O, Raabe GK, 2000. A critical review of cancer epidemiology in the petroleum industry, with a meta-analysis of a combined database of more than 350,000 workers. Regul. Toxicol. Pharmacol. 32, 78–98.

Yokota T, Sugawara K, Ito K, Takahashi R, Ariga H, Mizusawa H, 2003. Down regulation of DJ-1 enhances cell death by oxidative stress, ER stress, and proteasome inhibition. Biochem. Biophys. Res. Commun. 312, 1342–1348. [PubMed: 14652021]

Zhang L, Shimoji M, Thomas B, Moore DJ, Yu SW, Marupudi NI, Torp R, Torgner IA, Ottersen OP, Dawson TM, Dawson VL, 2005. Mitochondrial localization of the Parkinson's disease related protein DJ-1: implications for pathogenesis. Hum. Mol. Genet. 14, 2063–2073. [PubMed: 15944198]

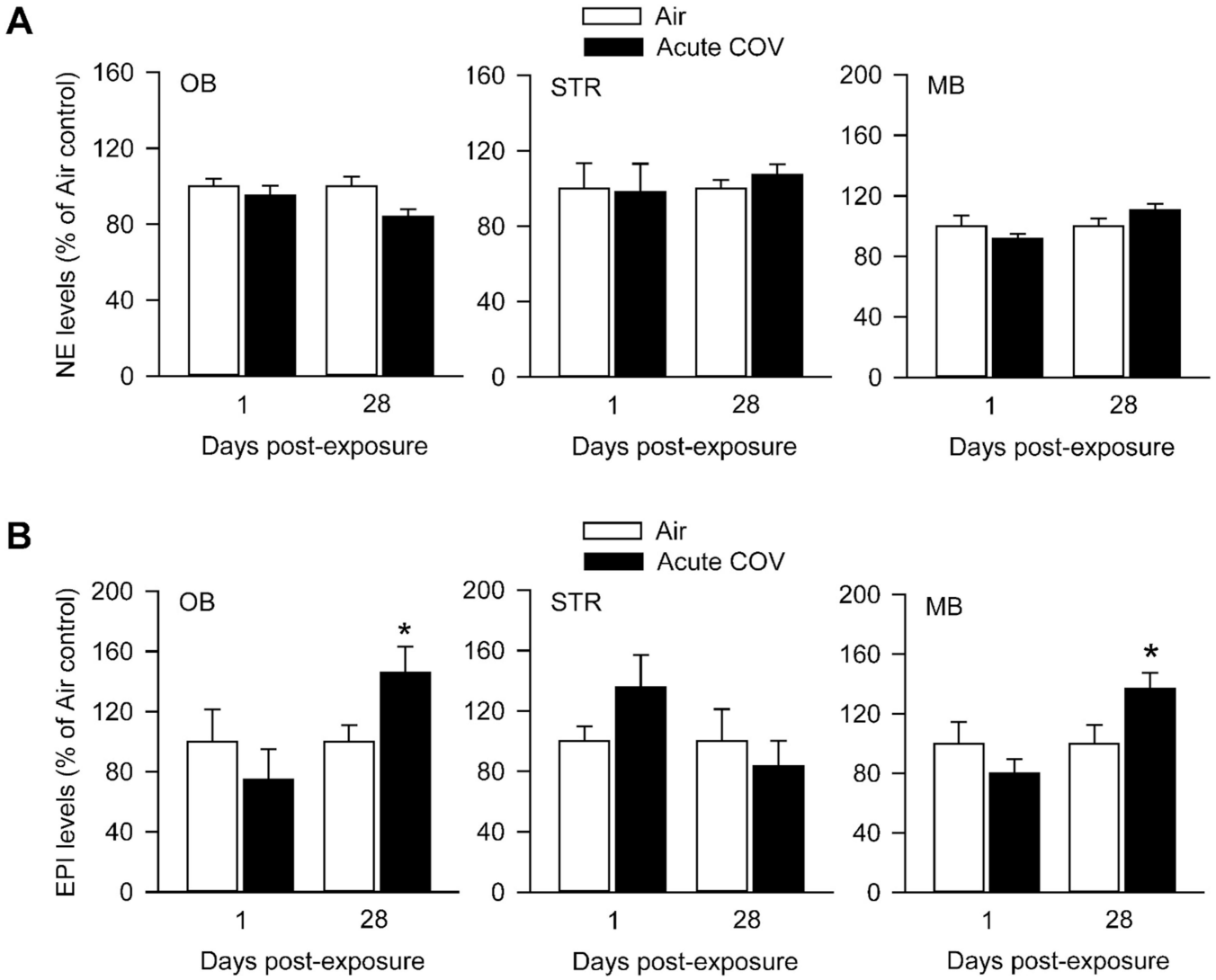

Fig. 1.

[**A**] Levels of Norepinephrine (NE) in discrete rat brain regions following acute crude oil vapor (COV) exposure. [**B**] Levels of Epinephrine (EPI) in discrete rat brain regions following acute COV exposure. Rats were exposed to an acute regimen of filtered air (□) or COV (■; 300 ppm; 6 h/d × 1 d) by whole-body inhalation. At 1 and 28 d post-exposure, the biogenic amine neurotransmitter was measured by HPLC-EC in the olfactory bulb (OB), and the dopaminergic brain regions, striatum (STR) and midbrain (MB). Following normalization to an internal standard, the neurotransmitter content was calculated from a standard curve. Values are expressed as percent of air-exposed controls (n = 8/group). * Indicates significant increase from the corresponding air-exposed controls ($P < 0.05$). # Indicates significant decrease from the corresponding air-exposed controls ($P < 0.05$). The quantified neurotransmitter content (ng/mg protein) are provided in the supplemental table S1.

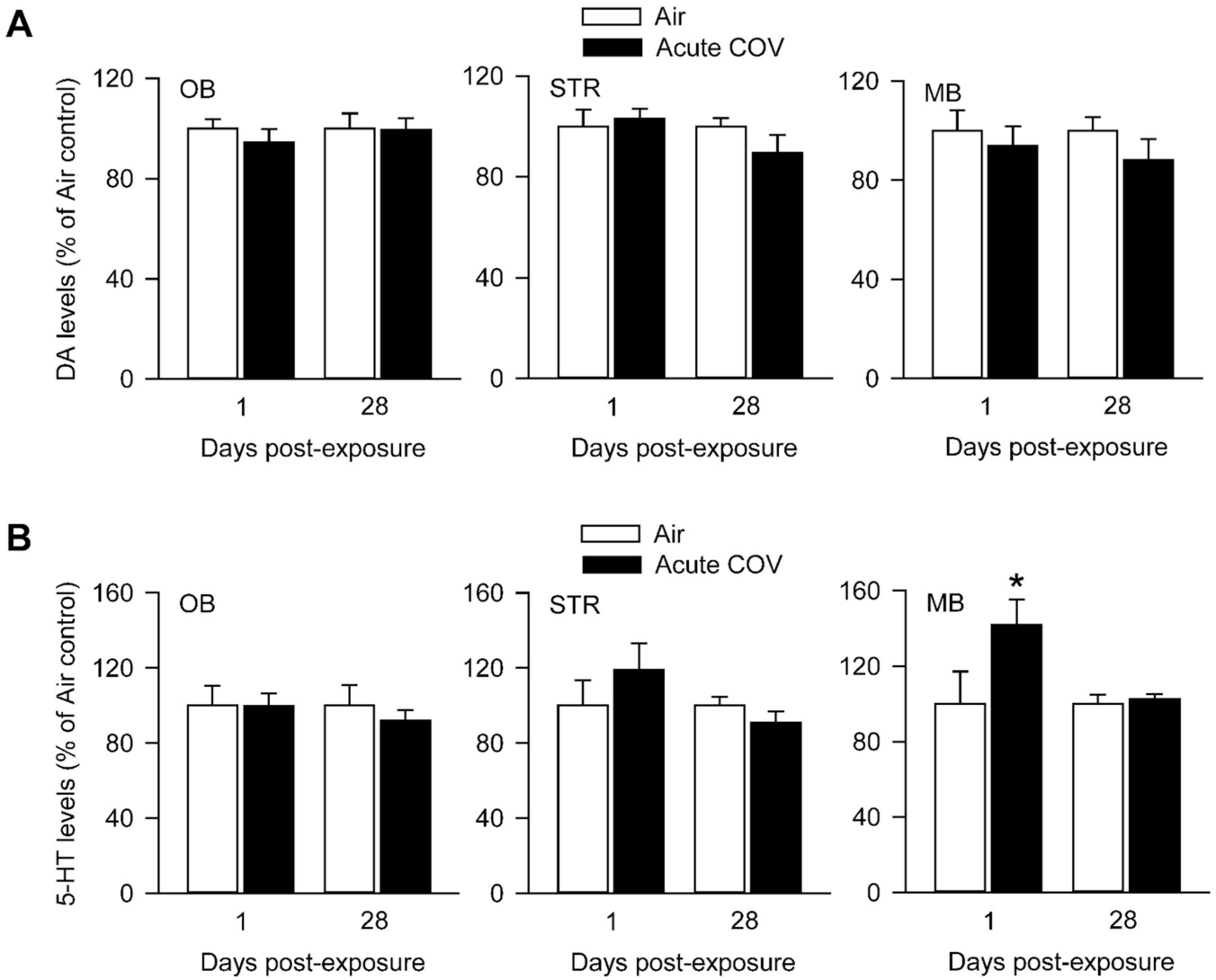

Fig. 2.

[**A**] Levels of Dopamine (DA) in discrete rat brain regions following acute COV exposure. [**B**] Levels of Serotonin (5-HT) in discrete rat brain regions following acute COV exposure. Rats were exposed to an acute regimen of filtered air (□) or COV (■; 300 ppm; 6 h/d × 1 d) by whole-body inhalation. At 1 and 28 d post-exposure, the biogenic amine neurotransmitter was measured by HPLC-EC in the olfactory bulb (OB), striatum (STR) and midbrain (MB). Following normalization to an internal standard, the neurotransmitter content was calculated using a standard curve. Values are expressed as percent of air-exposed controls (n = 8/group). * Indicates significant increase from the corresponding air-exposed controls ($P < 0.05$). # Indicates significant decrease from the corresponding air-exposed controls ($P < 0.05$). The quantified neurotransmitter content (ng/mg protein) are provided in the supplemental table S1.

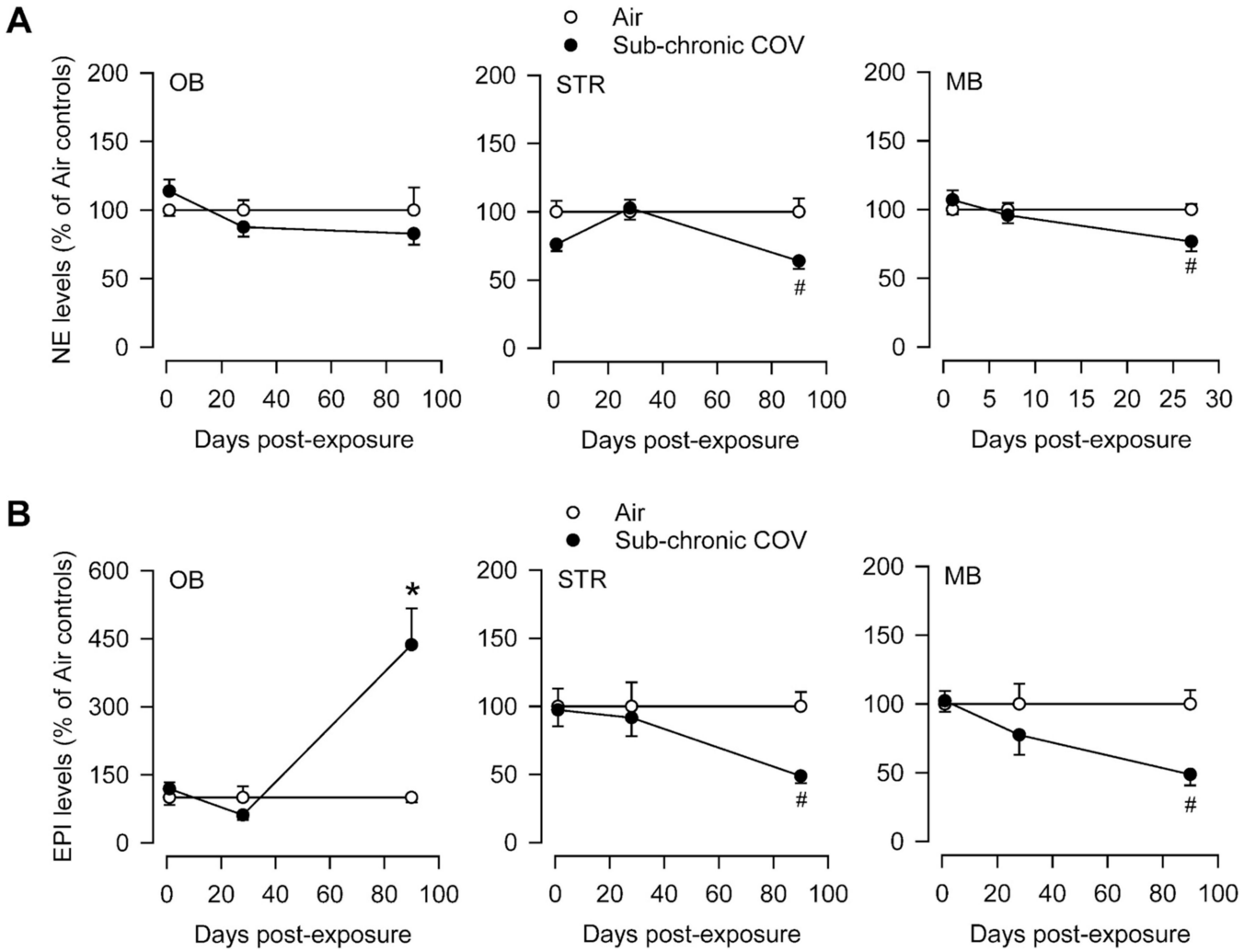

Fig. 3.

[**A**] Levels of Norepinephrine (NE) in discrete rat brain regions following sub-chronic COV exposure. [**B**] Levels of Epinephrine (EPI) in discrete rat brain regions following sub-chronic COV exposure. Rats were exposed to a sub-chronic regimen of filtered air (○) or COV (●; 300 ppm; 6 h/d × 4 d/wk. x 4 wks; total of 16 days) by whole-body inhalation. At 1, 28 d or 90 d post-exposure, the biogenic amine neurotransmitter was measured by HPLC-EC in the olfactory bulb (OB), striatum (STR) and midbrain (MB). Following normalization to an internal standard, the neurotransmitter content was calculated from a standard curve. Values are expressed as percent of air-exposed controls (n = 8/group). * Indicates significant increase from the corresponding air-exposed controls ($P < 0.05$). # Indicates significant decrease from the corresponding air-exposed controls ($P < 0.05$). The quantified neurotransmitter content (ng/mg protein) are provided in the supplemental table S4.

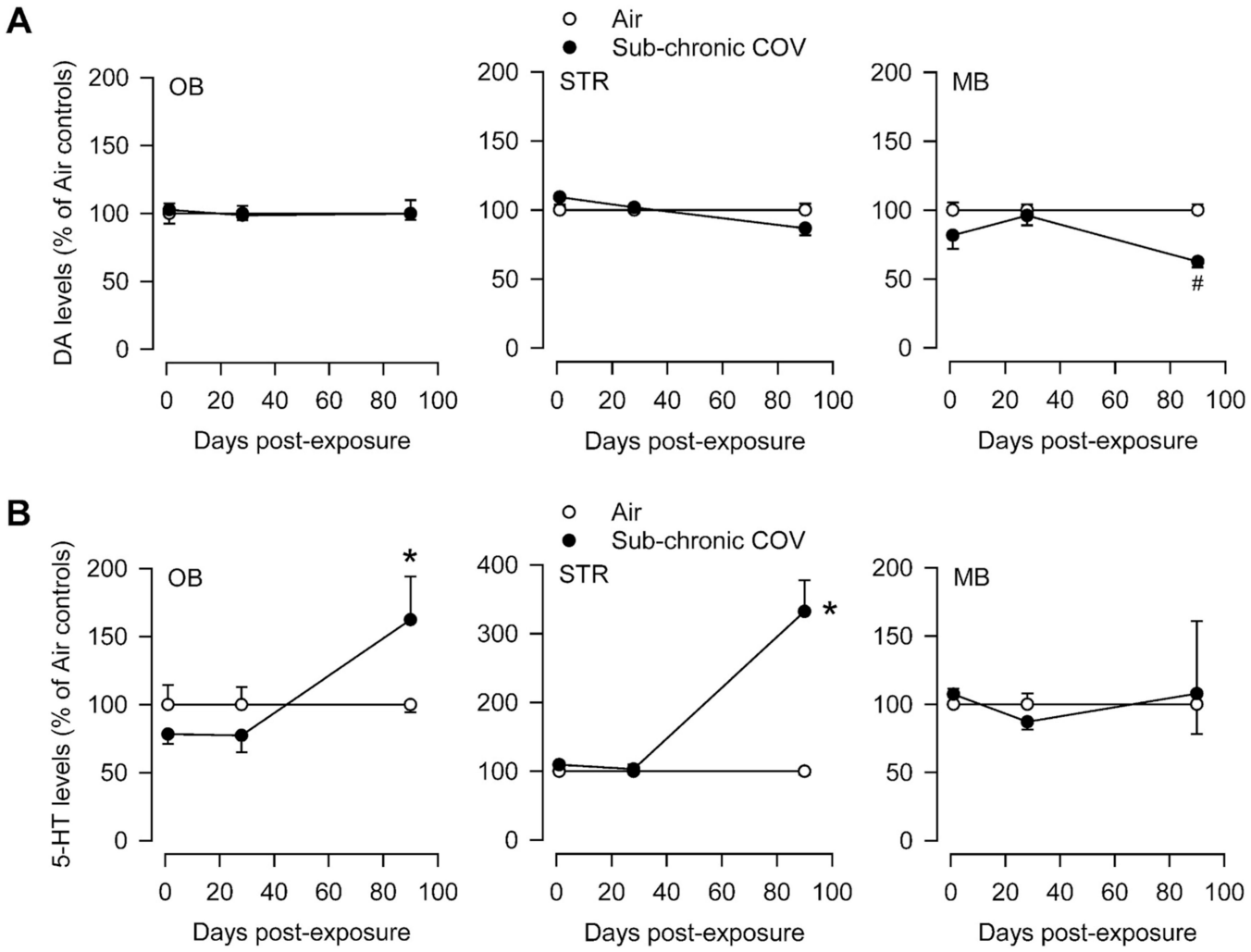

Fig. 4.

[**A**] Levels of Dopamine (DA) in discrete rat brain regions following sub-chronic COV exposure. [**B**] Levels of Serotonin (5-HT) in discrete rat brain regions following sub-chronic COV exposure. Rats were exposed to a sub-chronic regimen of filtered air (○) or COV (●; 300 ppm; 6 h/d × 4 d/wk. x 4 wks; total of 16 days) by whole-body inhalation. At 1, 28 d or 90 d post-exposure, the biogenic amine neurotransmitter was measured by HPLC-EC in the olfactory bulb (OB), striatum (STR) and midbrain (MB). Following normalization to an internal standard, the neurotransmitter content was calculated from a standard curve. Values are expressed as percent of air-exposed controls (n = 8/group). * Indicates significant increase from the corresponding air-exposed controls ($P < 0.05$). # Indicates significant decrease from the corresponding air-exposed controls ($P < 0.05$). The quantified neurotransmitter content (ng/mg protein) are provided in the supplemental table S4.

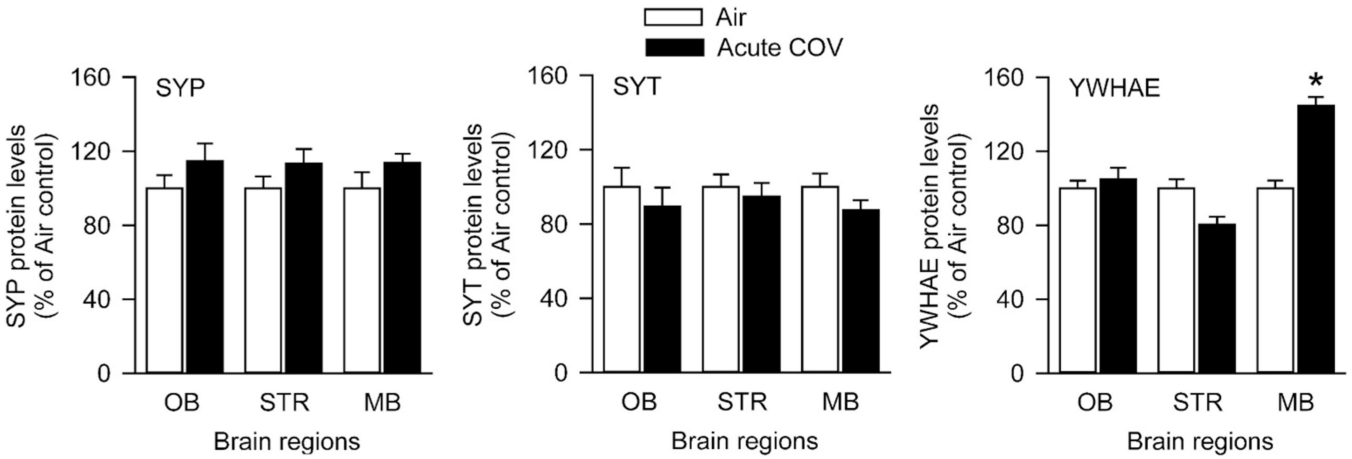

Fig. 5.

Changes in synaptic proteins in discrete rat brain regions following acute COV exposure. Rats were exposed to an acute regimen of filtered air (□) or COV (■; 300 ppm; 6 h/d × 1 d) by whole-body inhalation. At 28 d post-exposure, the protein expression of Synaptophysin 1 (SYP), Synaptotagmin 1 (SYT), and Tyrosine 3-monooxygenase/tryptophan 5-monooxygenase activation protein epsilon (14–3– 3E / YWHAE) were determined by western immunoblotting in the olfactory bulb (OB), striatum (STR) and midbrain (MB). Following normalization to the endogenous control β-actin (ACTB), the change in protein expression was calculated and expressed as percent of air-exposed controls (n = 8/group). * Indicates significant increase from the corresponding air-exposed controls ($P < 0.05$). # Indicates significant decrease from the corresponding air-exposed controls ($P < 0.05$).

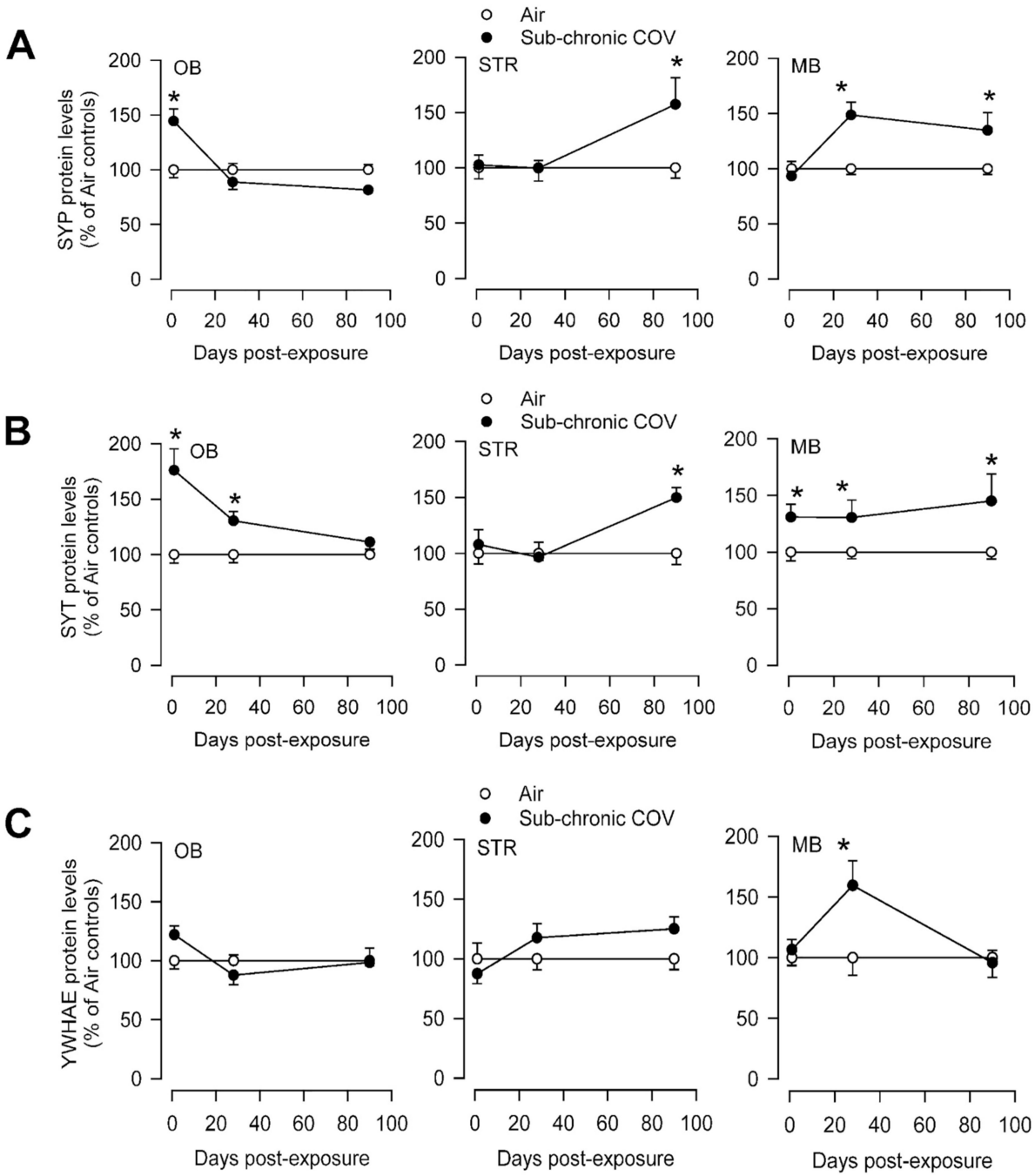

Fig. 6.

[A] Changes in Synaptophysin 1 (SYP) protein expression in discrete rat brain regions following sub-chronic COV exposure. [**B**] Changes in Synaptotagmin 1 (SYT) protein expression in discrete rat brain regions following sub-chronic COV exposure. [**C**] Changes in Tyrosine 3-monooxygenase/tryptophan 5-monooxygenase activation protein epsilon (14–3–3E/YWHAE) protein expression in discrete rat brain regions following sub-chronic COV exposure. Rats were exposed to a sub-chronic regimen of filtered air (○) or COV (●; 300 ppm; 6 h/d × 4 d/wk. x 4 wks; total of 16 days) by whole-body inhalation. At 1, 28 d or

90 d post-exposure, the protein expression was determined by western immunoblotting in the olfactory bulb (OB), striatum (STR) and midbrain (MB). Following normalization to the endogenous control β-actin (ACTB), the change in protein expression was calculated and expressed as percent of air-exposed controls (n = 8/group). * Indicates significant increase from the corresponding air-exposed controls ($P < 0.05$). # Indicates significant decrease from the corresponding air-exposed controls ($P < 0.05$).

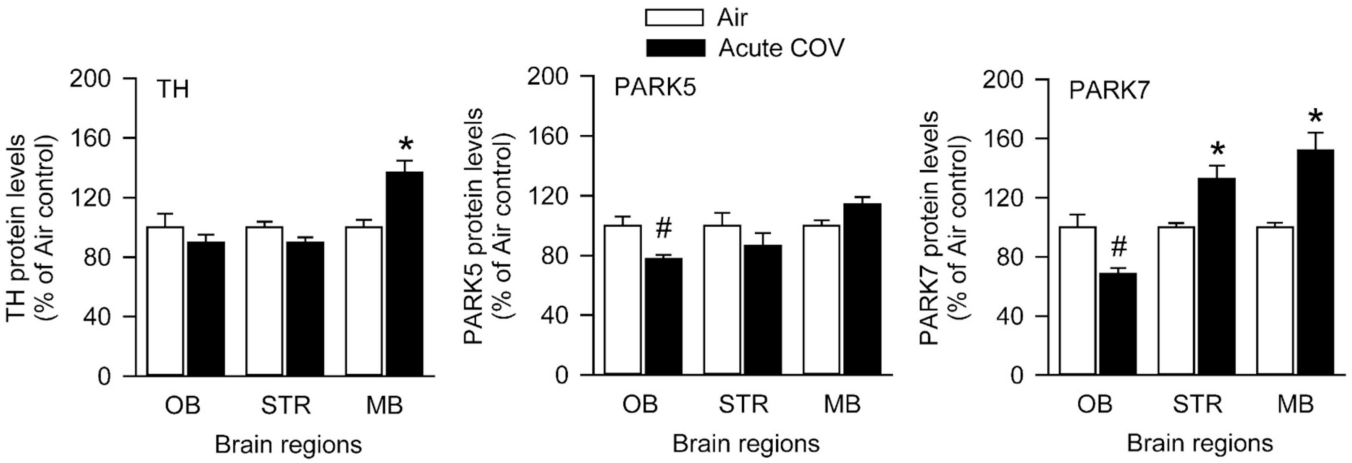

Fig. 7.

Changes in Parkinson's disease (PD)-related proteins in discrete rat brain regions following acute COV exposure. Rats were exposed to an acute regimen of filtered air (□) or COV (■; 300 ppm; 6 h/d × 1 d) by whole-body inhalation. At 28 d post-exposure, the protein expression of Tyrosine hydroxylase (TH), Ubiquitin Carboxyl-Terminal Esterase L1 (UCHL1/PARK5), and Parkinson's disease [Autosomal Recessive, Early Onset] 7 (PARK7) were determined by western immunoblotting in the olfactory bulb (OB), striatum (STR) and midbrain (MB). Following normalization to the endogenous control β-actin (ACTB), the change in protein expression was calculated and expressed as percent of air-exposed controls (n = 8/group). * Indicates significant increase from the corresponding air-exposed controls ($P < 0.05$). # Indicates significant decrease from the corresponding air-exposed controls ($P < 0.05$).

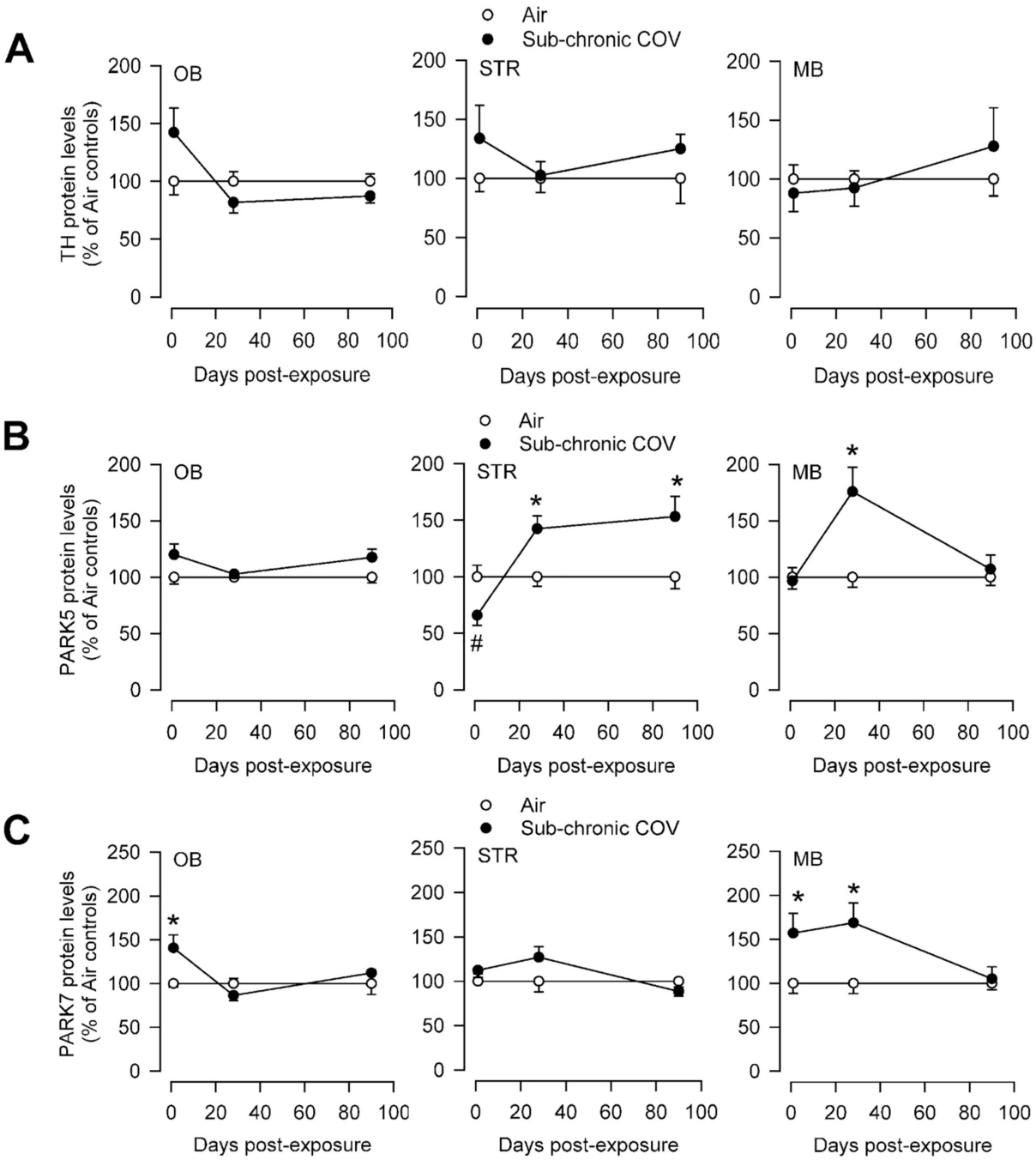

Fig. 8.

[**A**] Changes in Tyrosine hydroxylase (TH) protein expression in discrete rat brain regions following sub-chronic COV exposure. [**B**] Changes in Ubiquitin Carboxyl-Terminal Esterase L1 (UCHL1/PARK5) protein expression in discrete rat brain regions following sub-chronic COV exposure. [**C**] Changes in Parkinson's disease [Autosomal Recessive, Early Onset] 7 (PARK7) protein expression in discrete rat brain regions following sub-chronic COV exposure. Rats were exposed to a sub-chronic regimen of filtered air (○) or COV (●; 300 ppm; 6 h/d × 4 d/wk. x 4 wks; total of 16 days) by whole-body inhalation. At 1, 28 d or

90 d post-exposure, the protein expression was determined by western immunoblotting in the olfactory bulb (OB), striatum (STR) and midbrain (MB). Following normalization to the endogenous control β-actin (ACTB), the change in protein expression was calculated and expressed as percent of air-exposed controls (n = 8/group). * Indicates significant increase from the corresponding air-exposed controls ($P < 0.05$). # Indicates significant decrease from the corresponding air-exposed controls ($P < 0.05$).

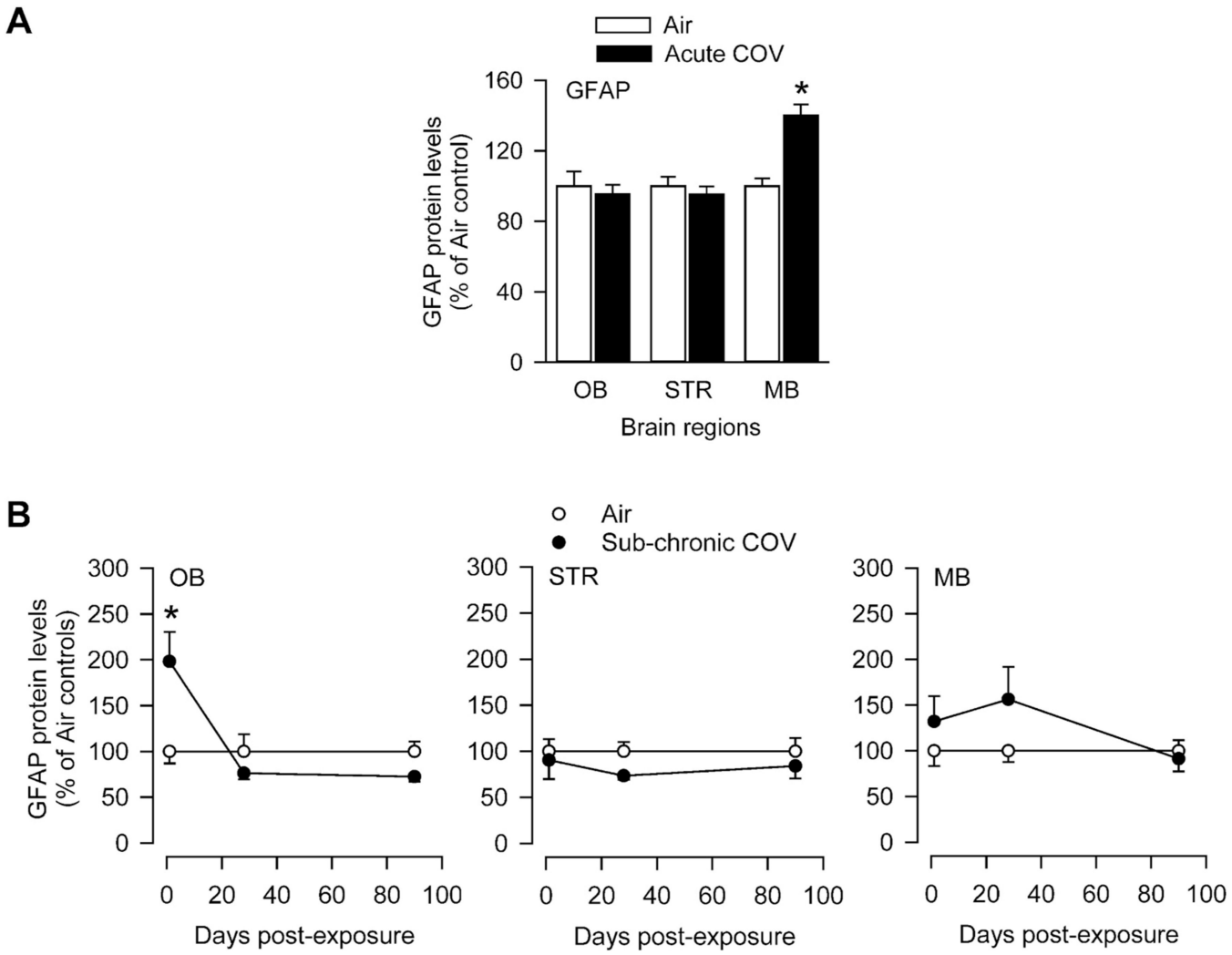

Fig. 9.

[**A**] Changes in astroglial marker protein, glial fibrillary acidic protein (GFAP), in discrete rat brain regions following acute COV exposure. Rats were exposed to an acute regimen of filtered air (□) or COV (■; 300 ppm; 6 h/d × 1 d) by whole-body inhalation. At 28 d post-exposure, the protein expression of GFAP was determined by western immunoblotting in the olfactory bulb (OB), striatum (STR) and midbrain (MB). Following normalization to the endogenous control β-actin (ACTB), the change in protein expression was calculated and expressed as percent of air-exposed controls (n = 8/group). * Indicates significant increase from the corresponding air-exposed controls ($P < 0.05$). # Indicates significant decrease from the corresponding air-exposed controls ($P < 0.05$). [**B**] Changes in glial fibrillary acidic protein (GFAP) protein expression in discrete rat brain regions following sub-chronic COV exposure. Rats were exposed to a sub-chronic regimen of filtered air (○) or COV (●; 300 ppm; 6 h/d × 4 d/wk. x 4 wks; total of 16 days) by whole-body inhalation. At 1, 28 d or 90 d post-exposure, the protein expression of GFAPwas determined by western immunoblotting in the olfactory bulb (OB), striatum (STR) and midbrain (MB). Following normalization to the endogenous control β-actin (ACTB), the change in protein expression was calculated and

expressed as percent of air-exposed controls (n = 8/group). * Indicates significant increase from the corresponding air-exposed controls ($P < 0.05$). # Indicates significant decrease from the corresponding air-exposed controls ($P < 0.05$).